

Synthesis and Structure–Activity Relationships of 3-Aryloxindoles: A New Class of Calcium-Dependent, Large Conductance Potassium (Maxi-K) Channel Openers with Neuroprotective Properties

Piyasena Hewawasam,^{*,†} Matthew Erway,[†] Sandra L. Moon,[‡] Jay Knipe,[§] Harvey Weiner,[‡] Christopher G. Boissard,[‡] Debra J. Post-Munson,[‡] Qi Gao,^{||} Stella Huang,[⊥] Valentin K. Gribkoff,[‡] and Nicholas A. Meanwell[†]

Departments of Chemistry, Neuroscience, Metabolism and Pharmacokinetics, Analytical Research and Development, and Discovery Analytical Sciences, The Bristol-Myers Squibb Pharmaceutical Research Institute, 5 Research Parkway, Wallingford, Connecticut 06492

Received April 25, 2001

A series of 3-aryloxindole derivatives were synthesized and evaluated as activators of the cloned maxi-K channel *mSlo* expressed in *Xenopus laevis* oocytes using electrophysiological methods. The most promising maxi-K openers to emerge from this study were (±)-3-(5-chloro-2-hydroxyphenyl)-1,3-dihydro-3-hydroxy-6-(trifluoromethyl)-2*H*-indol-2-one ((±)-**8c**) and its 3-des-hydroxy analogue (±)-**11b**. The individual enantiomers of (±)-**8c** were synthesized, and the maxi-K channel-opening properties were shown to depend on the absolute configuration of the single stereogenic center with the efficacy of (–)-**8c** superior to that of both (+)-**8c** and the racemic mixture when evaluated at a concentration of 20 μM. Racemic **11b** exhibited greater efficacy than either the racemic **8c** or the more active enantiomer in the electrophysiological evaluation. In vitro metabolic stability studies conducted with (±)-**8c** and (±)-**11b** in rat liver S9 microsomal fractions revealed significant oxidative degradation with two hydroxylated metabolites observed by liquid chromatography/mass spectrometry for each compound in addition to the production of **8c** from **11b**. The pharmacokinetic properties of (±)-**8c** and (±)-**11b** were determined in rats as a prelude to evaluation in a rat model of stroke that involved permanent occlusion of the middle cerebral artery (MCAO model). In the MCAO model, conducted in the spontaneously hypertensive rat, the more polar 3-hydroxy derivative (±)-**8c** did not demonstrate a significant reduction in cortical infarct volume when administered intravenously at doses ranging from 0.1 to 10 mg/kg as a single bolus 2 h after middle cerebral artery occlusion when compared to vehicle-treated controls. In contrast, intravenous administration of (±)-**11b** at a dose of 0.03 mg/kg was found to reduce the measured cortical infarct volume by approximately 18% when compared to vehicle-treated control animals. Intraperitoneal administration of (±)-**11b** at a dose of 10 mg/kg 2 h following artery occlusion was shown to reduce infarct volume by 26% when compared to vehicle-treated controls. To further probe the effects of compounds (±)-**8c** and (±)-**11b** on neurotransmitter release in vitro, both compounds were examined for their ability to reduce electrically stimulated [³H]-glutamate release from rat hippocampal slices that had been preloaded with [³H]-glutamate. Only (±)-**11b** was able to demonstrate a significant inhibition [³H]-glutamate release in this assay at a concentration of 20 μM, providing concordance with the profile of these compounds in the MCAO model. Although (±)-**11b** showed some promise as a potential developmental candidate for the treatment of the sequelae of stroke based on its efficacy in the rat MCAO model, the pharmacokinetic profile of this compound was considered to be less than optimal and was not pursued in favor of derivatives with enhanced metabolic stability.

Introduction

Stroke is presently recognized as the third leading cause of adult disability and death in the United States and Europe with an incidence in excess of 700 000 per year in the United States and over 2 million per annum worldwide.¹ Providing clinicians with effective drugs that provide stroke victims with protection against some

of the consequences of this devastating and debilitating event represents one of the most prominent unmet medical needs in the clinical arena. Strokes are classified into two types: ischemic stroke, which results from vessel occlusion, and hemorrhagic stroke, in which there is intracerebral hemorrhage resulting in neuronal damage. Hemorrhagic strokes represent approximately 20% of all such events but are very difficult to classify, leading to some caution when treating stroke victims with the thrombolytic agents that have been developed to facilitate dissolution of the occluding thrombus. These agents are utilized to restore blood flow to ischemic neuronal tissue, and tissue plasminogen activator has recently been approved for use in a limited patient

* To whom correspondence should be addressed. Tel.: (203)677-7815. Fax: (203)677-7702. E-mail: hewawasap@bms.com.

[†] Department of Chemistry.

[‡] Department of Neuroscience.

[§] Department of Metabolism and Pharmacokinetics.

^{||} Department of Analytical Research and Development.

[⊥] Department of Discovery Analytical Sciences.

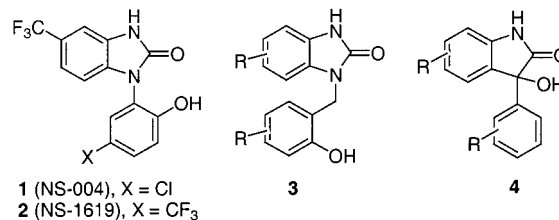
population.² In an effort to provide clinicians with effective neuroprotective therapies to be administered poststroke, numerous mechanistic approaches have been examined in the past decade including antagonists of AMPA/kainate^{3–5} and *N*-methyl-D-aspartate (NMDA) excitatory amino acid receptors⁶ and inhibitors of neuronal adenosine reuptake.^{7,8} However, to date, none of these potential neuroprotective agents have succeeded due to either a lack of demonstrated clinical efficacy or poor side effect profiles,⁹ resulting in the current situation in which there is no approved neuroprotective therapy. We have approached the problem of poststroke neuroprotection by developing potent and specific openers of large conductance, Ca²⁺-activated (maxi-K) potassium channels. This strategy is designed to protect neurons by enhancing an intrinsic mechanism of cell regulation that should ultimately reduce abnormally high levels of Ca²⁺ entry,^{10,11} thereby reducing the release of potentially pathogenic neurotransmitters¹² and controlling neuronal hyperexcitability.¹³

Background and Rationale

Potassium channels have emerged as interesting targets for drug discovery based on their structural diversity, tissue distribution, and regulatory role in cell function, thereby providing an opportunity to design drugs that target specific K⁺ channels that may selectively intervene in a wide range of physiological processes and disease states. Because they are subject to regulation by a range of physiological factors including voltage, the metabolic state of a cell, intracellular Ca²⁺ concentration, and receptor-activated processes,^{14,15} they play a critical role in regulating cell membrane potential and neuronal excitability.^{16–19} The Ca²⁺-activated potassium (K_{Ca}) channel subfamily is characterized by their dependence on the intracellular concentration of Ca²⁺ ions for activity but are also regulated by transmembrane voltage and phosphorylation state.²⁰ K_{Ca} channels have been further subdivided based on channel conductance into three distinct categories: the large conductance maxi-K or BK channels are those that exhibit a single channel conductance of greater than 150 picoSiemens (pS) while intermediate conductance and low conductance channels are categorized as 50–150 pS and less than 50 pS, respectively. Maxi-K channels are of particular interest because of their large channel conductance and their expression in a range of excitable cell types, including neurons and smooth muscle cells.^{20,21} In view of this and as a consequence of their central role in regulating cell activity, modulators of maxi-K channels are potentially useful agents for the treatment of a variety of disease states associated with both the central nervous system and smooth muscle function.^{22,23}

The opening of maxi-K channels is stimulated by an increase in intracellular Ca²⁺; openers of these channels augment this opening of the channel by Ca²⁺. As a consequence, the pharmacological modulation of channel function is largely dependent on the presence of high levels of intracellular Ca²⁺, a circumstance encountered during neuronal ischemia.^{10–11,23} Maxi-K channel opening stimulated by Ca²⁺ in the presence of a pharmacological opener would function to limit further Ca²⁺ entry, thus interrupting the cascade of events leading to ischemic neuronal death that is initiated by abnor-

Chart 1. Structures of NS-004 (**1**), NS-1619 (**2**), *N*-Benzylated Benzimidazol-2-one Derivatives (**3**), and 3-Aryl-3-hydroxyoxindoles (**4**)



mally high Ca²⁺ entry. Because intracellular levels of Ca²⁺ are low in nonischemic tissue, a maxi-K opener would not be expected to significantly affect channels under these circumstances, thereby reducing the potential for undesirable side effects.

The range of synthetic and naturally occurring compounds that demonstrate maxi-K channel-opening activity and their associated electrophysiological and biochemical pharmacological properties has recently been reviewed.^{22,23} The benzimidazolone derivatives NS 004 (**1**) and NS 1619 (**2**) are prominent prototypes among the small molecule openers of maxi-K channels^{24–26} that have been studied in some detail, both in vitro and in vivo.^{27–30} A recent study of the structurally homologous *N*-benzylated benzimidazol-2-one derivatives (**3**) has illuminated fundamental aspects of this maxi-K-opening pharmacophore and provided the first insights into structure–activity relationships (Chart 1).³¹

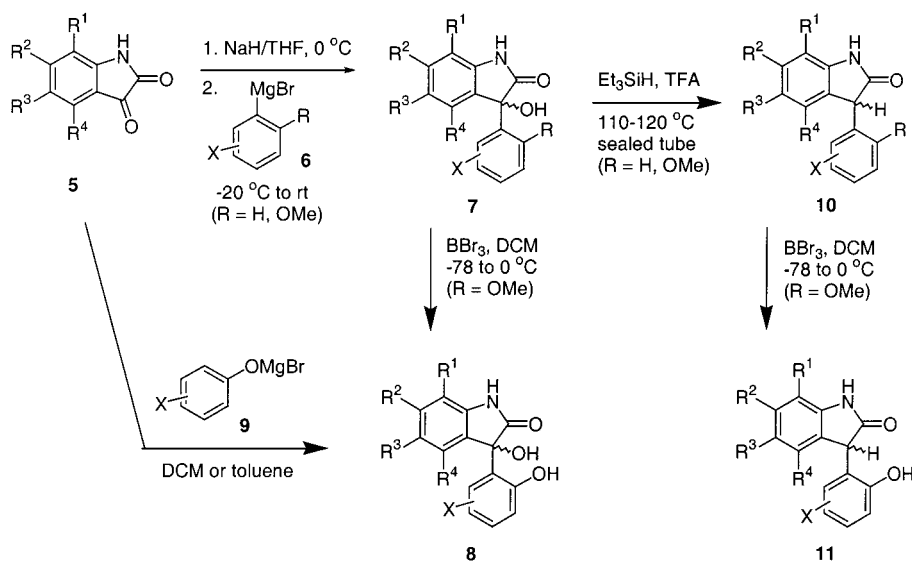
As part of a broad-based effort directed toward the identification of potent and selective activators of neuronal maxi-K channels that would be useful as neuroprotective agents, we recently disclosed a structurally novel class of maxi-K channel openers based upon 3-aryl-3-hydroxyoxindoles (**4**).³² More specifically, the maxi-K channel-opening activity of 3-(5-chloro-2-hydroxyphenyl)-1,3-dihydro-3-hydroxy-6-(trifluoromethyl)-2*H*-indol-2-one (**8c**) was described and shown to be dependent upon the absolute configuration at the stereogenic center. In this paper, a more detailed analysis of structure–activity relationships associated with the BK-opening pharmacophore inherent to **8c** is presented. In addition, the potential of **8c** and its analogues to function as neuroprotective agents, as predicted by demonstration of neuroprotective effects in the middle cerebral artery occlusion (MCAO) rat model of stroke, is described.

Chemistry

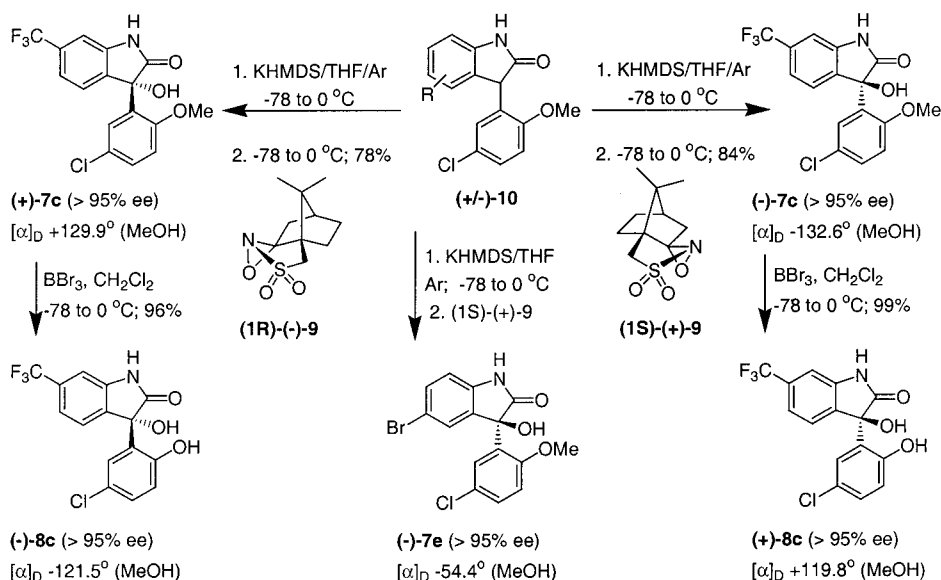
The racemic 3-aryl-3-hydroxyindol-2-ones (**7** or **8**) were prepared in a straightforward fashion from the corresponding isatins **5**,³³ as depicted in Scheme 1. The addition of an aryl Grignard reagent (**6**) to the sodium salt of an isatin **5** in tetrahydrofuran (THF) afforded the corresponding 3-aryl-3-hydroxyindol-2-ones **7** in 80–95% yields. For derivatives of **7** substituted with a methoxy moiety, demethylation was accomplished using BBr₃ in CH₂Cl₂ to provide the corresponding phenols **8**.

A more direct approach to phenol derivatives was developed that relied upon the reaction of magnesium phenolates (**9**), prepared by treating phenols with ethylmagnesium bromide, with isatins **5** in either CH₂Cl₂

Scheme 1



Scheme 2



or toluene,³⁴ as summarized in Scheme 1. Although it was anticipated that only electron-rich magnesium phenolates would react efficiently with isatins **5**, this reaction proved to be quite general and a variety of electron-deficient magnesium phenolates coupled effectively to afford adducts **8**. Moreover, meta-substituted magnesium phenolates were found to react with isatins **5** with excellent regioselectivity, affording only those adducts in which the phenol was substituted at the least-hindered of the two ortho positions. However, the steric interactions that underlie this selectivity prevented the reaction of **5** with meta-disubstituted magnesium phenolates, which reacted only poorly. As a consequence, tractable products could not be isolated.

Several of the 3-aryl-3-hydroxyoxindoles **7** were reduced to the corresponding 3-aryloxindoles **10**, as shown in Scheme 1. Dehydroxylation was accomplished by heating **7** in a sealed tube with an excess of Et₃SiH in CF₃CO₂H at 110–120 °C. As might be anticipated, the rate of this dehydroxylation reaction was dependent upon the electronic nature of the substituents present on the oxindole aromatic ring of **7**. Thus, unsubstituted

and electron-rich oxindoles were deoxygenated much more rapidly than oxindoles substituted with electron-withdrawing moieties. Demethylation of the methyl ether moiety of **10** with BBr₃ in CH₂Cl₂ provided the corresponding phenols **11** (Scheme 2).

The dehydroxylated oxindole derivatives were viewed as potential precursors to homochiral 3-aryl-3-hydroxyoxindoles by way of the asymmetric hydroxylation reaction developed by Davis,³⁵ as depicted in Scheme 2.³² Treating the racemic indolone **10c** with potassium bis(trimethylsilyl)amide in THF at -78 °C under an atmosphere of argon followed by the addition of the chiral oxaziridine, (1*R*)-(-)-**9** afforded only racemic **7c**, as determined by ¹H nuclear magnetic resonance (NMR) in the chiral solvent (*L*)-trifluoromethylphenyl carbinol.³⁶ In this solvent, the CH₃O protons of the two enantiomers of racemic **7c** resonated at δ 3.49 and 3.47 ppm. It was subsequently determined that the potassium salt of **10c** was extremely sensitive to oxidation by oxygen dissolved in THF. Consequently, the reaction was repeated using dry degassed THF. Under these circumstances, oxidation of the potassium salt of **10c** with (1*S*)-

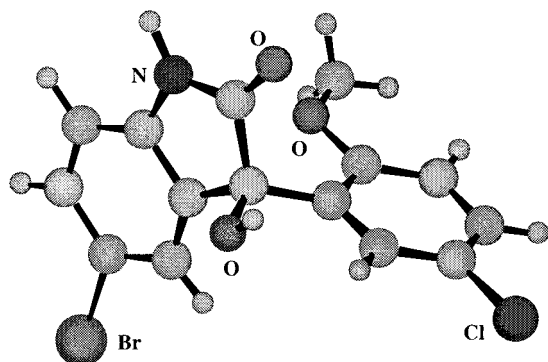


Figure 1. X-ray structure of (3*R*)-(-)-5-bromo-3-(5-chloro-2-methoxyphenyl)-1,3-dihydro-3-hydroxy-2*H*-indol-2-one ((-)-**7e**) showing the atomic labeling scheme.

(+)-**9** at $-78\text{ }^{\circ}\text{C}$ followed by gradual warming to $0\text{ }^{\circ}\text{C}$ and quenching with glacial acetic acid gave the desired 3-hydroxyindolone (-)-**7c**. The enantiomeric purity of (-)-**7c** was determined to be $>95\%$ after examination of the ^1H NMR spectrum in the chiral solvent (*L*)-trifluoromethylphenyl carbinol.³⁶ When the reaction was repeated with (1*R*)-(-)-**9**, the opposite enantiomer, (+)-**7c**, was obtained, again in $>95\%$ ee. Because suitable single crystals of either enantiomer (+)-**7c** or (-)-**7c** could not be obtained, (3*R*)-(-)-5-bromo-3-(5-chloro-2-methoxyphenyl)-1,3-dihydro-3-hydroxy-2*H*-indol-2-one ((-)-**7e**) was prepared in an analogous fashion (Scheme 2), using (1*S*)-(+)-**9** as the oxidant, and the absolute configuration was determined by single crystal X-ray analysis. The solid state structure of this compound is shown in Figure 1. In analogy with this stereochemical assignment, the absolute configurations of (+)-**7c** and (-)-**7c** are tentatively assigned as depicted in Scheme 2. Finally, the ether moieties of (+)-**7c** and (-)-**7c** were demethylated by exposure to BBr_3 in CH_2Cl_2 to afford the corresponding phenols (-)-**8c** and (+)-**8c**, respectively. The compounds prepared by these methods are compiled in Table 1 along with relevant physicochemical data.

Results and Discussion

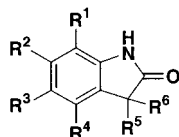
The effect of the target compounds on outward K^+ current was determined by using a two electrode voltage clamp recording from *Xenopus laevis* oocytes expressing cloned *mSlo*³⁷ (or *hSlo*³⁸) maxi-K channels, as described previously.³⁹ The voltage clamp protocols consisted of 500–750 ms voltage steps in +20 mV increments from a holding potential of -60 to $+140$ mV, which were conducted in the absence and presence of test compound. Compounds under evaluation were maintained at a concentration of $20\text{ }\mu\text{M}$ in the recording chamber, and all experiments were concluded by incubation of the oocytes for 10 min with 50 nM iberiotoxin (IbTx). Voltage clamp protocols in the presence of this selective blocker of the maxi-K channel allowed quantification of *mSlo* or *hSlo* current expression. In all cases, a minimum of five different oocytes was used to evaluate the effect of a single drug concentration on channel current, and for each compound tested, the average percentage change in *mSlo* (or *hSlo*) IbTx sensitive current relative to drug-free control (100%) was determined. The results obtained are presented in Table 1 along with data for NS-004 (**1**), which allows the efficacy

of the oxindole derivatives to be compared with a prototypical maxi-K channel opener.

The structure–activity relationships described in Table 1 provide a basic understanding of the oxindole maxi-K channel-opening pharmacophore, extending the findings of the earlier study, which was restricted to 3-hydroxy oxindole derivatives. In addition to identifying the optimal substitution patterns associated with the heterocycle and 3-phenyl moieties, the data in Table 1 further illuminate the effect of asymmetry on maxi-K-opening efficacy and reveal some subtle differences between this chemotype and the benzylated benzimidazolones reported earlier.³¹ From the limited structure–activity data associated with the 3-des-hydroxy series, compounds **10b** and **11a,b**, it appears that an electron-withdrawing substituent is not an essential structural element since the prototype **11a** demonstrates efficacy comparable to NS-004 (**1**). However, as observed with the benzimidazolone chemotype,³¹ the introduction of the 6- CF_3 group (**11b**) markedly enhances channel-opening efficacy, results that taken together are indicative of greater intrinsic activity in this series. Compound **11b** also provided an opportunity to evaluate one aspect of the contribution of the phenol moiety by methylation, which eliminates the potential to function as a hydrogen bond donor. While the significantly attenuated efficacy of ether **10b** as compared to **11b** may be compatible with this suggestion, a deleterious effect associated with increased steric bulk cannot be disregarded.

The 3-hydroxy oxindoles were the major focus of this study and subject to a more extensive structure–activity survey that included an evaluation of the effects of chirality on channel-opening properties. The latter was examined in the context of prototypes methyl ether **7c** and the derived phenol **8c**, a pair of compounds that provided contrasting results. Ether **7c** exhibited modest efficacy that was not dependent on the absolute configuration at C-3 while the racemic phenol **8c** more effectively enhanced channel conductance, extending the trend seen between **10b** and **11b**, but in a fashion sensitive to the identity of the single stereogenic center. Thus, the channel-opening activity of (-)-**8c** was superior to that of both (+)-**8c** and the racemic mixture. The aqueous solubility properties of (\pm)-**8c** were such that evaluation at the higher concentration of $30\text{ }\mu\text{M}$ was permitted. In this experiment, a dose-related increase in the efficacy of channel opening was observed with an increase in outward current in oocytes expressing *mSlo* to $200.8 \pm 17.8\%$ of control. Unfortunately, attempts to evaluate the individual enantiomers of **8c** at a concentration of $30\text{ }\mu\text{M}$ were unsuccessful due to precipitation of the test compound under the assay conditions.

A more detailed electrophysiological evaluation of (\pm)-**8c** was conducted using an inside-out excised patch from a COS cell expressing *mSlo*. In this assay, (\pm)-**8c** significantly increased the mean open time and reduced periods of closure of *mSlo* maxi-K channels at a concentration as low as 100 nM (Figure 2A). The effects of (\pm)-**8c** on the human maxi-K channel *hSlo* expressed in HEK cells were also examined (Figure 2B). In both systems, (\pm)-**8c** was found to increase the probability of the open state of the channels at a concentration of $1\text{ }\mu\text{M}$.

Table 1. Structure and Physical Properties of 3-Substituted 1,3-Dihydro-indol-2-one Derivatives and Effect on Maxi-K-Mediated Outward Current in *Xenopus laevis* Oocytes Expressing Cloned Maxi-K Channels

compd no.	R ¹	R ²	R ³	R ⁴	R ⁵	R ⁶	method of preparation	mp (°C) ^a	% increase in <i>mSlo</i> current at 20 μM	molecular formula
1 (NS-004)									132 ± 13 ^b	
7a	H	CF ₃	H	H	C ₆ H ₅	OH	A	247–249	87 ± 4	C ₁₅ H ₁₀ F ₃ NO ₂
7b	H	CF ₃	H	H	3-Cl-C ₆ H ₄	OH	A	268–270	97 ± 6 ^b	C ₁₅ H ₉ ClF ₃ NO ₂
(±)- 7c	H	CF ₃	H	H	2-OCH ₃ , 5-Cl-C ₆ H ₃	OH	A	207–210	120 ± 7 ^b	C ₁₆ H ₁₁ ClF ₃ NO ₃
(+)- 7c	H	CF ₃	H	H	2-OCH ₃ , 5-Cl-C ₆ H ₃	OH	scheme 2	243–245	117 ± 3 ^b	C ₁₆ H ₁₁ ClF ₃ NO ₃
(-)- 7c	H	CF ₃	H	H	2-OCH ₃ , 5-Cl-C ₆ H ₃	OH	scheme 2	244–245	116 ± 4 ^b	C ₁₆ H ₁₁ ClF ₃ NO ₃
7d	H	H	CF ₃	H	2-OCH ₃ , 5-Cl-C ₆ H ₃	OH	A	218–220	109 ± 3	C ₁₆ H ₁₁ ClF ₃ NO ₃
(-)- 7e	H	H	Br	H	2-OCH ₃ , 5-Cl-C ₆ H ₃	OH	scheme 2	257–259	NT	C ₁₅ H ₁₁ BrClNO ₃
8a	H	H	H	H	2-OH, 5-Cl-C ₆ H ₃	OH	C	216–218	95 ± 3	C ₁₄ H ₁₀ ClNO ₃ ·0.4H ₂ O
8b	H	CF ₃	H	H	2-OH-C ₆ H ₄	OH	C	209–211	90 ± 3	C ₁₅ H ₁₀ F ₃ NO ₃
(±)- 8c	H	CF ₃	H	H	2-OH, 5-Cl-C ₆ H ₃	OH	A and B	210–213	131 ± 7	C ₁₅ H ₉ ClF ₃ NO ₃
(+)- 8c	H	CF ₃	H	H	2-OH, 5-Cl-C ₆ H ₃	OH	scheme 2	200–201	123 ± 11	C ₁₅ H ₉ ClF ₃ NO ₃
(-)- 8c	H	CF ₃	H	H	2-OH, 5-Cl-C ₆ H ₃	OH	scheme 2	198–200	141 ± 9	C ₁₅ H ₉ ClF ₃ NO ₃
8d	H	H	CF ₃	H	2-OH, 5-Cl-C ₆ H ₃	OH	A and B	156–158	108 ± 8	C ₁₅ H ₉ ClF ₃ NO ₃
8e	CF ₃	H	H	H	2-OH, 5-Cl-C ₆ H ₃	OH	A and B	205–207	122 ± 7	C ₁₅ H ₉ ClF ₃ NO ₃
8f	H	H	H	CF ₃	2-OH, 5-Cl-C ₆ H ₃	OH	A and B	239–242	127 ± 13	C ₁₅ H ₉ ClF ₃ NO ₃
8g	H	H	NO ₂	H	2-OH, 5-Cl-C ₆ H ₃	OH	C	215–217	78 ± 5	C ₁₄ H ₉ ClN ₂ O ₅ ·0.5H ₂ O
8h	H	H	CH ₃	H	2-OH, 5-Cl-C ₆ H ₃	OH	C	225–227	100 ± 3	C ₁₅ H ₁₂ ClNO ₃
8i	H	H	F	H	2-OH, 5-Cl-C ₆ H ₃	OH	C	158–161	106 ± 6	C ₁₄ H ₉ ClFNO ₃
8j	H	Cl	H	Cl	2-OH, 5-Cl-C ₆ H ₃	OH	C	232–235	117 ± 8	C ₁₄ H ₈ Cl ₃ NO ₃
8k	H	CF ₃	H	CF ₃	2-OH, 5-Cl-C ₆ H ₃	OH	A and B	191–193	127 ± 9	C ₁₆ H ₈ ClF ₃ NO ₃
8l	H	CF ₃	H	H	2-OH, 5-F-C ₆ H ₃	OH	C	184–186	97 ± 7	C ₁₅ H ₉ F ₄ NO ₃
8m	H	CF ₃	H	H	2-OH, 5-Br-C ₆ H ₃	OH	C	194–196	89 ± 3	C ₁₅ H ₉ BrF ₃ NO ₃ ·0.25H ₂ O
8n	H	CF ₃	H	H	2-OH, 5-I-C ₆ H ₃	OH	C	192–194	107 ± 7	C ₁₅ H ₉ F ₃ INO ₃
8o	H	CF ₃	H	H	2-OH, 5-CH ₃ -C ₆ H ₃	OH	C	226–228	106 ± 4	C ₁₆ H ₁₂ F ₃ NO ₃
8p	H	CF ₃	H	H	2-OH, 5-C ₆ H ₅ -C ₆ H ₃	OH	C	180–185	106 ± 3	C ₂₁ H ₁₄ F ₃ NO ₃
8q	H	CF ₃	H	H	2-OH-C ₁₀ H ₆	OH	C	159–160	116 ± 4	C ₁₉ H ₁₂ F ₃ NO ₃ ·0.85H ₂ O
8r	H	CF ₃	H	H	2-OH, 4-NH ₂ -C ₆ H ₃	OH	C	276–280	92 ± 2	C ₁₅ H ₁₁ F ₃ N ₂ O ₃
8s	H	CF ₃	H	H	2-OH, 5-OCH ₃ -C ₆ H ₃	OH	C	231–233	81 ± 7	C ₁₆ H ₁₂ F ₃ NO ₄
8t	H	CF ₃	H	H	2-OH, 5-(NCH ₃ -piperaziny)C ₆ H ₃	OH	C	210–215	91 ± 2	C ₂₀ H ₂₀ F ₃ N ₃ O ₃
8u	H	CF ₃	H	H	2-OH, 5-CF ₃ -C ₆ H ₃	OH	C	175–177	130 ± 11	C ₁₆ H ₉ F ₆ NO ₃
8v	H	CF ₃	H	H	2-OH, 4-CF ₃ -C ₆ H ₃	OH	C	198–201	108 ± 7	C ₁₆ H ₉ F ₆ NO ₃
8w	H	CF ₃	H	H	2-OH, 3-Cl-C ₆ H ₃	OH	C	202–205	116 ± 5	C ₁₅ H ₉ ClF ₃ NO ₃
8x	H	CF ₃	H	H	2-OH, 4-Cl-C ₆ H ₃	OH	C	188–190	93 ± 6	C ₁₅ H ₉ ClF ₃ NO ₃
8y	H	CF ₃	H	H	2-OH, 4,5-diCl-C ₆ H ₂	OH	C	152–154	107 ± 5	C ₁₅ H ₈ Cl ₂ F ₃ NO ₃ ·0.1H ₂ O
8z	H	CF ₃	H	H	2-OH, 3,5-diCl-C ₆ H ₂	OH	C	210–212	108 ± 6	C ₁₅ H ₈ Cl ₂ F ₃ NO ₃
8za	H	CF ₃	H	H	2-OH, 4-NH ₂ -5-Cl-C ₆ H ₂	OH	C	198–200	94 ± 4	C ₁₅ H ₁₀ ClF ₃ N ₂ O ₃
8zb	H	CF ₃	H	H	2-OH, 3-I, 5-Cl-C ₆ H ₂	OH	see exptl	210–212	124 ± 4	C ₁₅ H ₈ ClF ₃ INO ₃
10b	H	CF ₃	H	H	2-OCH ₃ , 5-Cl-C ₆ H ₃	H	D	210–213	110 ± 0	C ₁₆ H ₁₁ ClF ₃ NO ₂
11a	H	H	H	H	2-OH, 5-Cl-C ₆ H ₃	H	D and B	256–258	139 ± 6	C ₁₄ H ₁₀ ClNO ₂
11b	H	CF ₃	H	H	2-OH, 5-Cl-C ₆ H ₃	H	D and B	266–268	164 ± 8	C ₁₅ H ₉ ClF ₃ NO ₂

^a All new compounds exhibited spectroscopic and combustion data in accord with the designated structure. ^b Compounds **1** (NS-004), **7b**, (±)-**7c**, (+)-**7c**, and (-)-**7c** were shown to have identical effects on *mSlo*- and *hSlo*-mediated BK currents.³⁹

The optimal regiochemistry for the heterocyclic CF₃ substituent was determined by comparing the activity of **8c** with its isomers **8d–f**. It is clear from the data in Table 1 that a 6-CF₃ moiety is superior to the 5-CF₃ isomer, in the context of both a methyl ether (**7d**) and a phenol (**8d**) as the 3-aryl element. However, efficacy is largely restored with the 7- and 4-substituted CF₃ isomers **8e** and **8f**, respectively, and maintained although not enhanced with the C-6, C-4 disubstitution pattern found in **8k**. None of the remaining aromatic substituents examined (**8g–j**) that complete this survey afforded active compounds.

The maxi-K channel-opening properties of this chemotype also exhibited sensitivity to the identity and pattern of substitution of the 3-aryl element. Of particular note and in contrast to the benzylated benzimidazolone series, removal of the 5-Cl atom (**8b**) afforded

an inactive compound. Somewhat remarkably, activity was not restored by substitution at the 5-position by either F, Br, or I, since compounds **8l–n** are ineffective openers of the *mSlo* channel. The chloro-substituted regioisomers **8w** and **8x** were also inactive, but a 5-CF₃ moiety, compound **8u**, was found to be compatible with good efficacy although, again, the 5-position is optimal in this limited series, as demonstrated by the lack of channel-opening activity associated with **8v**. Further underscoring the uniqueness of the 5-Cl substituent, introduction of additional halogens provides inactive derivatives **8y** and **8z**. In addition, a 2-hydroxyl or 2-methoxyl moiety also appears to be a critical aspect of the pharmacophore since **7b** and **7a** are also ineffective channel openers.

Several additional substituents appended to the 3-phenyl ring were introduced in an effort not only to

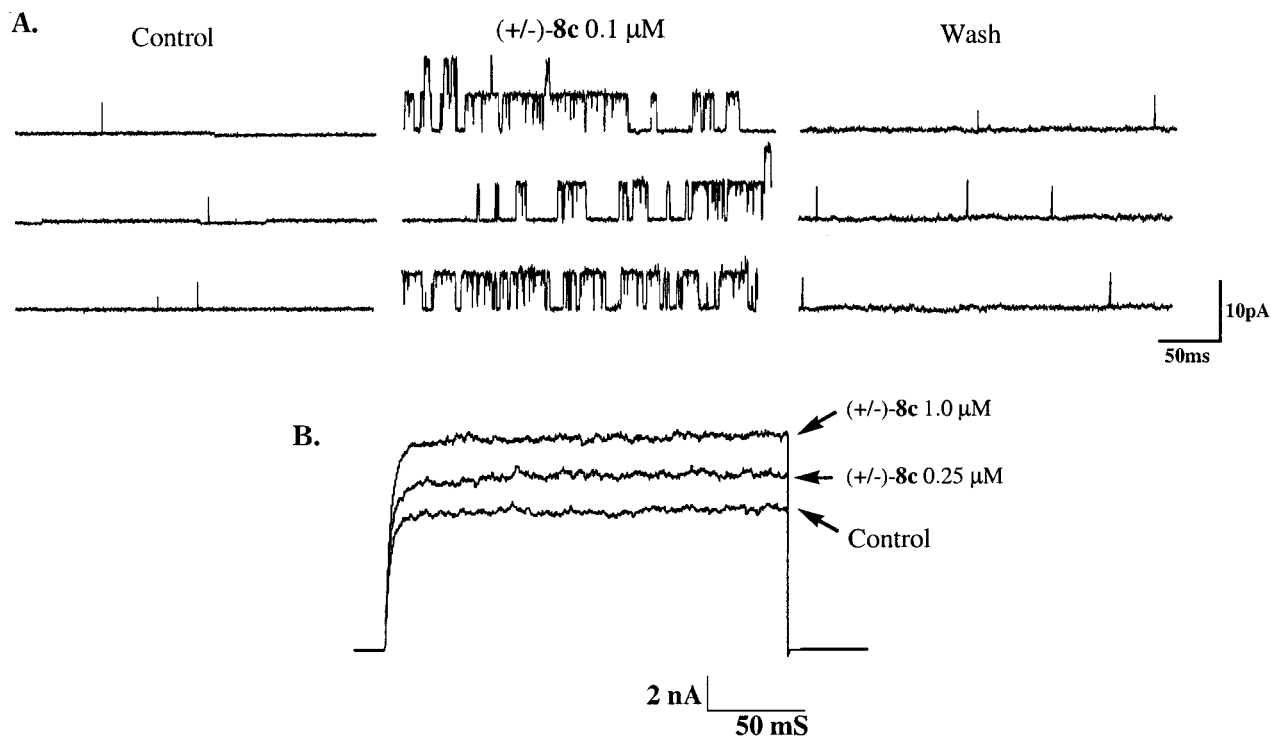


Figure 2. (A) Example of an inside-out excised patch from a COS cell expressing *mSlo*. The channel open probability was very low in control medium, and application of (\pm)-**8c** (0.1 μ M; 2 min) produced a rapid and reversible large increase in channel opening. The holding potential was +20 mV, and the calcium concentration at the intracellular patch face was 3 mM. (B) Whole cell recording of the effects of (\pm)-**8c** on the human maxi-K channel *hSlo* expressed in HEK cells. The compound produced a concentration-dependent increase in maxi-K channel-mediated outward current elicited by +30 mV voltage steps from a holding potential of -60 mV. The pipet calcium concentration was 1.0 mM.

Table 2. Whole Brain and Plasma Concentrations of (\pm)-**8c** and (\pm)-**11b** after IV Administration (4.6 mg/kg) to Male Rats

compd	plasma level ^a		brain level ^b		mean brain/plasma ratio	
	0.25 hr	2 hr	0.25 hr	2 hr	0.25 hr	2 hr
(\pm)- 8c	1.2 \pm 0.2	0.231 \pm 0.004	1.34 \pm 0.06	0.87 \pm 0.05	1.1	3.8
(\pm)- 11b	3.3 \pm 0.3	0.28 \pm 0.01	2.4 \pm 0.2	0.23 \pm 0.01	0.73	0.82

^a Concentration as μ g/mL; mean of three animals \pm standard deviation. ^b Concentration as μ g/g wet weight; mean of three animals \pm standard deviation.

probe structure–activity relationships but also to enhance aqueous solubility. However, none of the substituents examined provided compounds (**8r**, **8t**, and **8za**) with significant channel-opening activity, reinforcing the sensitivity of this region of the pharmacophore to the nature and pattern of substitution. The structure–activity pattern that has emerged for the 3-aryloxindole class of maxi-K channel openers indicates a pharmacophore highly sensitive to structural variation with optimal activity restricted to a pattern of substitution largely identified with two benzimidazolone prototypes NS-004 (**1**) and NS-1619 (**2**).

Metabolism and Pharmacokinetics

As a prelude to evaluating compounds in animal models of stroke, the pharmacokinetic properties of the most promising maxi-K openers (\pm)-**8c** and (\pm)-**11b** were examined in rats, with particular attention focused on determining the extent of brain penetration following intravenous administration. Table 2 shows the plasma and whole brain concentrations of each compound at 15 min and 2 h after IV dosing. Brain levels of (\pm)-**11b** exceeded those of (\pm)-**8c** at 15 min, but by 2 h, (\pm)-**8c** concentrations were greater than those of (\pm)-**11b**,

Table 3. Mean Whole Brain and Plasma Pharmacokinetic Parameters of (\pm)-**8c** after IV Administration (4.6 mg/kg) to Rats^a

param	plasma	brain	brain/plasma ratio ^c
C_{max} (ng/g)		1.4	
T_{max} (hr)		0.25	
AUC ^b	1.9	4.8	2.5
$T_{1/2}$ (hr)	2.5	3.4	

^a Male rats (24) were dosed, and three animals were killed at each of eight time points after dosing. ^b Expressed as μ g hr/mL for plasma and μ g hr/g for brain calculated by the trapezoidal rule over 0–8 h after dosing. ^c On the basis of ratio of AUC values.

suggesting a prolonged elimination of (\pm)-**8c** from brain tissue. To more fully explore the relationship between brain and plasma levels of (\pm)-**8c** over time, a larger group of rats was administered (\pm)-**8c** intravenously and whole brain and plasma concentrations were determined out to 8 h postdosing. The results from this expanded study (Table 3) verified that (\pm)-**8c** rapidly entered rat brain after IV administration and attained concentrations there that exceeded those of plasma (a total brain/plasma AUC ratio of 2.5, evaluated over 8 h). Furthermore, (\pm)-**8c** was eliminated somewhat more slowly from rat brain than from plasma (elimination half-lives of 3.4 and 2.5 h, respectively).

Table 4. Percent Reduction of Neocortical Infarct Volume in Rats (IV Administration 2 h Post-MCAO)^a

compd	study (group)	dose (mg/kg)								
		vehicle	0.005	0.01	0.03	0.1	0.3	1.0	5.0	10.0
(±)- 8c	A									
	percent mean					4%		10%	10%	4%
	(SE)	168.5				161.8		152.2	151.0	161.0
	<i>n</i>	(8.3)				(8)		(6.4)	(8)	(5.3)
(±)- 11b	A									
	percent mean				18% ^b	9%		0%	6%	toxic
	(SE)	162.3			133.1	147.7		163.1	152.6	
	<i>n</i>	(6.7)			(9.1)	(8.7)		6.4	(6.2)	
	B									
	percent mean		4%	-7% (increase)	12% ^b					
(SE)	154.3	148.8	165.4	135.4						
	<i>n</i>	(6.3)	(8.8)	(7.7)	(6.5)					
lubeluzole	A									
	percent mean						13% ^c	22% ^b	18% ^b	
	(SE)	180.9					157.5	141.1	148.3	
	<i>n</i>	(8.3)					(5.3)	(8.6)	(5.6)	
		9	9	9	9		9	9	9	

^a Neocortical infarct volume in mm³ expressed as group mean (with standard error). Percent reduction as compared to vehicle-treated controls from the same study. ^b $p \leq 0.01$, Student's *t* test or ANOVA and Dunnett's *t* test. ^c $p \leq 0.02$, Student's *t* test or ANOVA and Dunnett's *t* test.

When incubated with a rat liver S9 preparation, both (±)-**8c** and (±)-**11b** were metabolized. Over 1 h, 39% of (±)-**8c** was metabolized to two monohydroxylated metabolites, detected by liquid chromatography (LC)/mass spectrometry (MS) profiling, while 76% of (±)-**11b** was metabolized to at least three monohydroxylated metabolites, one of which was identified as (±)-**8c**.⁴⁸

Effects of (±)-**8c** and (±)-**11b** on Models of Permanent Focal Infarct in the Rat

Because both (±)-**8c** and (±)-**11b** demonstrated adequate brain penetration in rats, they were evaluated in a model of focal stroke that involved a permanent occlusion of the middle cerebral artery (MCAO model) conducted in the spontaneously hypertensive rat (SHR). This procedure results in a reliably large neocortical infarct volume that is measured by means of vital dye exclusion in serial slices of the brain harvested 24 h after initiating arterial occlusion. In this protocol, compounds were administered intravenously or intraperitoneally 2 h postocclusion in order to mimic a clinical situation in which patients present to the hospital with significant delay after experiencing a stroke. This protocol also provides a stringent test for the ability of drug candidates to confer protection to neuronal tissue.

In this model, the more polar 3-hydroxy derivative (±)-**8c** did not show a significant reduction in cortical infarct volume when administered intravenously at doses ranging from 0.1 to 10 mg/kg as a single bolus 2 h after MCAO when compared to vehicle-treated (2% dimethyl sulfoxide (DMSO), 98% propylene glycol) controls (Table 4). However, perhaps reflecting its greater brain-penetrating ability, (±)-**11b** demonstrated activity in this model of cerebral ischemia, as shown in Tables 4 and 5. Intravenous administration of (±)-**11b** at a dose of 0.03 mg/kg reduced the measured cortical infarct volume by approximately 18% as compared to control (Table 4). Intraperitoneal administration of (±)-**11b** at a dose of 10 mg/kg 2 h following artery occlusion

Table 5. Neocortical Infarct Volume in Rats and Percent Reduction^a after Administration of (±)-**11b** (Intraperitoneal Administration 2 h Post-MCAO)

study	dose of (±)- 11b (mg/kg)			
	vehicle	5	10	20
A				
percent mean		6%	26% ^b	
(SE)	171.4	161.8	127.3	
<i>n</i>	(7.0)	(6.5)	(5.0)	
	9	9	9	
B				
percent mean			24% ^b	9%
(SE)	149.0		113.2	135.5
<i>n</i>	(6.2)		(8.3)	(4.7)
	11		8	7

^a Neocortical infarct volume in mm³ expressed as group mean (with standard error). Percent reduction as compared to vehicle-treated controls from the same study. ^b $p \leq 0.01$, Student's *t* test or ANOVA and Dunnett's *t* test.

reduced infarct volume by 26% when compared to vehicle-treated control (Table 5). Under these conditions, the extent of neuroprotection demonstrated by (±)-**11b** was either equivalent or superior to a range of experimental neuroprotectants that possess diverse mechanisms of action. For comparison, the noncompetitive NMDA receptor antagonist Cerestat⁴⁰ (CN1102, Cambridge Neuroscience) was inactive in this model, a result consistent with the poor performance of this compound in clinical trials. However, lubeluzole,⁴¹ which is thought to affect the glutamate/nitric oxide synthase pathway, showed efficacy comparable to (±)-**11b**, with a 22% reduction in infarct volume (Table 4).

One possible explanation for the inactivity of the hydroxyl analogue (±)-**8c** may be that this compound did not achieve adequate brain levels at early time points when compared to (±)-**11b**. As a general observation but for reasons not clearly apparent, we have found that maxi-K openers with a brain concentration of ≥ 2000 ng/g at 15 min following administration of a dose of 5 mg/kg show significant activity in MCAO stroke model.⁴² However, given the complex profile of (±)-**11b** in the MCAO model of stroke, the narrow dosing

Table 6. Effect of Maxi-K Channel Openers (\pm)-**8c** and (\pm)-**11b** on Electrically Stimulated [^3H]-Glutamate Release in Hippocampal Slices In Vitro

compd	concn (μM)	electrically stimulated [^3H]-glutamate release (% control) ^a
(\pm)- 8c	1	89 \pm 5 (4)
	20	93 \pm 7 (5)
(\pm)- 11b	20	71 \pm 8 (5)

^a The results are the mean \pm SEM with the number of experiments given in parentheses.

window for efficacy, and the observation that both compounds enter brain tissue, alternate explanations were sought.

As part of an effort to illuminate further reasons for the differences in performance of (\pm)-**8c** and (\pm)-**11b**, the effects of the compounds on neurotransmitter release in vitro were examined. While the experiments with either *mSlo* or *hSlo* channels expressed in oocytes described above provide a clear understanding of the effects of (\pm)-**8c** and (\pm)-**11b** on a specifically configured K^+ channel, the biochemical pharmacological effects under the more complex circumstances of neurotransmitter release in vitro proved to be instructive. This setting provides a more realistic evaluation of the performance of the compounds under conditions in which the maxi-K channels are configured in a more natural fashion. The amino acid glutamate mediates much of the excitatory synaptic transmission in the brain and is thought to be a key mediator in the process of learning. However, excess glutamate release has also been implicated in disease states such as epilepsy and ischemic brain damage, damaging neurons in the latter by initiating a cascade of events that lead to cell death.¹² Because ischemia-related damage maybe reduced by limiting glutamate release, compounds (\pm)-**8c** and (\pm)-**11b** were evaluated for their ability to interfere with electrically stimulated [^3H]-glutamate release in an in vitro assay. Briefly, this assay is performed using rat hippocampal slices, which are preloaded with [^3H]-glutamate. Electrical stimulation evokes the release of [^3H]-glutamate, and the synaptic pool of this neurotransmitter is approximately 50% of the total released during stimulation, as estimated by the effects of total pharmacological synaptic blockade. As shown in Table 6, only (\pm)-**11b** was able to demonstrate a significant inhibition of electrically stimulated [^3H]-glutamate release in vitro at a concentration of 20 μM . One possible explanation for the differences between compounds (\pm)-**11b** and (\pm)-**8c** is that the latter compound, as the hydroxylated derivative of (\pm)-**11b**, is more hydrophilic, which may limit its penetration into the tissue wedges. This possibility is consistent with the results of brain penetration studies, which demonstrated that (\pm)-**8c** reached lower initial levels in the brain in vivo when compared to (\pm)-**11b** at 0.25 h (Table 2). Alternatively, the maxi-K channels expressed naturally in rat hippocampal slices may be configured such that the biochemical pharmacological effects of (\pm)-**8c** do not reflect the channel-opening effects observed with the cloned channels in oocytes. Finally, the possibility that the additional hydroxyl present in (\pm)-**8c** leads to additional pharmacological activities that override the effects of maxi-K channel opening cannot be excluded.

Conclusion

In summary, we have identified a novel class of maxi-K channel openers and demonstrated that channel-opening activity is sensitive to both the nature and the pattern of substitution of both aromatic elements as well as the absolute configuration of an asymmetric center. The preliminary structure–activity data for this series indicate the importance of both an electron-withdrawing substituent on the oxindole nucleus and the presence of a phenolic hydroxyl for effective expression of BK channel-opening properties. The 3-aryl oxindole (\pm)-**11b** showed promise as a potential candidate for further development based on its in vitro and in vivo profiling. However, because of its metabolic instability, particularly hydroxylation at the 3-position of the heterocycle, further development of (\pm)-**11b** as a neuroprotective agent for the treatment of stroke was not pursued in favor of derivatives with a more favorable pharmacokinetic profile.^{43,49}

Experimental Section

Melting points were recorded on a Thomas-Hoover capillary apparatus and are uncorrected. Magnetic resonance (NMR) spectra were recorded on a Bruker AM FT instrument operating at 300 MHz for proton (^1H) and 75 MHz for carbon (^{13}C) or a Varian Gemini 300 operating at 300 MHz for proton (^1H). All spectra were recorded using tetramethylsilane (TMS) as an internal standard, and signal multiplicity was designated according to the following abbreviations: s = singlet, d = doublet, t = triplet, q = quartet, m = multiplet, brd s = broad singlet. Infrared (IR) spectra were obtained using a Nicolet MX1 FT spectrometer, scanning from 4000 to 400 cm^{-1} , and calibrated to the 1601 cm^{-1} absorption of a polystyrene film. Optical rotations were determined on a Perkin-Elmer 41 polarimeter in the solvents indicated. Low-resolution mass spectra and the apparent molecular ion (MH^+) or ($\text{M} - \text{H}$) $^-$ were determined on a Finnigan TSQ 7000. Analytical samples were dried in vacuo at 78 $^\circ\text{C}$ or in the presence of P_2O_5 at room temperature for at least 12 h. Elemental analyses were provided by Bristol-Myers Squibb's Analytical Chemistry Department. For those compounds whose elemental analyses were not performed, approximate purity was determined to be $>95\%$ by NMR.

Method A. Grignard Addition to Isatins (Scheme 1). General Procedure. A solution of aryl Grignard reagent (**6**, 1–2 equiv) in THF was added to a stirred cold ($-20\text{ }^\circ\text{C}$) solution of the Na salt of the isatin in THF under an atmosphere of N_2 . The mixture was allowed to warm to room temperature and stirred until the isatin was consumed, typically 1–2 h. The reaction mixture was diluted with ether, cooled in an ice-bath, and then quenched with 1 N HCl. The organic layer was separated, washed with 0.5 N NaOH, water, and brine, and then dried (Na_2SO_4). The crude solid isolated after evaporation of the solvents was triturated with CH_2Cl_2 to afford pure 1,3-dihydro-3-hydroxy-3-aryl-2*H*-indol-2-one derivatives (**7**) in 80–95% yield.

Method B. Demethylation of Arylmethyl Ether (Scheme 1). General Procedure. Demethylation of the methyl ether moiety of **7** or **10** was carried out using BBr_3 in CH_2Cl_2 . To a cold ($-78\text{ }^\circ\text{C}$), stirred solution of **7** ($\text{R} = \text{OMe}$) or **10** ($\text{R} = \text{OMe}$) in anhydrous CH_2Cl_2 , BBr_3 (3 equiv, 1 M solution in CH_2Cl_2) was added under an atmosphere of N_2 . The mixture was subsequently stirred in an ice bath until starting material disappeared by thin-layer chromatography (TLC; typically 1–2 h). The reaction mixture was quenched with saturated NaHCO_3 and acidified with 1 N HCl. Where the product was soluble in CH_2Cl_2 , the organic layer was separated, washed with brine, and then dried (MgSO_4). For products insoluble in CH_2Cl_2 , the organic layer was evaporated at room temperature and the aqueous residue was extracted with EtOAc. The extract was washed with brine, dried over

Na₂SO₄, and concentrated in vacuo to give **8** or **11**, respectively. The crude products were purified either by trituration with CH₂Cl₂ or recrystallization from EtOAc/hexanes to afford pure product in 80–95% yield.

Method C. Addition of Magnesium Phenolates to Isatins (Scheme 1). General Procedure. A solution of EtMgBr (1.1 equiv) in THF was added dropwise to a cold (0 °C) solution of the phenol (1.2 equiv) in anhydrous THF. The resultant white suspension of bromomagnesium phenolate was concentrated to dryness using a rotary evaporator, the residue was dissolved in anhydrous CH₂Cl₂, and the isatin (1 equiv) was added as a solid. The reaction was performed at room temperature with progress monitored by TLC. In those cases where no reaction was observed at ambient temperature, the reaction mixture was heated at reflux until the isatin was consumed before it was cooled to room temperature. The reaction mixtures were quenched with 1 N HCl, and the organic layer was separated and washed with water and brine before it was dried over MgSO₄. The crude products remaining after concentration were purified by either flash column chromatography or recrystallization to afford pure 1,3-dihydro-3-hydroxy-2-(2-hydroxyaryl)-2H-indol-2-ones (**8**).

Method D. Dehydroxylation of 3-Aryl-3-hydroxyoxindoles 7 (Scheme 1). General Procedure. A mixture of **7** (1 equiv), Et₃SiH (3 equiv), and CF₃CO₂H (3 equiv) was heated at 110–120 °C in a sealed tube for 1–3 days until deoxygenation was complete. Excess Et₃SiH and CF₃CO₂H were evaporated, and the residue was subjected to flash chromatography (silica gel/3% MeOH in CH₂Cl₂) to afford the desired deoxygenated product **10** in yields ranging from 80 to 90%.

(±)-1,3-Dihydro-3-hydroxy-3-phenyl-6-(trifluoromethyl)-2H-indol-2-one (**7a**). mp 247–249 °C. ¹H NMR (DMSO-*d*₆): δ 6.85 (1H, s), 7.12 (1H, s), 7.24–7.34 (7H, m), 10.70 (1H, s). MS: *m/e* 294 (MH⁺). Anal. (C₁₅H₁₀F₃NO₂) H, N; C: calcd, 61.44; found, 60.96.

(±)-3-(3-Chlorophenyl)-1,3-dihydro-3-hydroxy-6-(trifluoromethyl)-2H-indol-2-one (**7b**). mp 268–270 °C. ¹H NMR (DMSO-*d*₆): δ 7.05 (1H, s), 7.06–7.09 (1H, m), 7.14 (1H, s), 7.31–7.41 (4H, m), 7.42 (1H, s), 10.80 (1H, s). MS: *m/e* 328 (MH⁺). Anal. (C₁₅H₉ClF₃NO₂) H, N; C: calcd, 54.98; found, 55.41.

(±)-3-(5-Chloro-2-methoxyphenyl)-1,3-dihydro-3-hydroxy-6-(trifluoromethyl)-2H-indol-2-one (**7c**). mp 207–210 °C. IR (KBr, cm⁻¹): 3400, 1730, 1320, 1250, 1125, 1170. ¹H NMR (DMSO-*d*₆): δ 3.41 (3H, s), 6.91 (1H, s), 6.94 (1H, d, *J* = 8.7 Hz), 7.05 (2H, m), 7.19 (1H, d, *J* = 8.2 Hz), 7.35 (1H, dd, *J* = 8.6 Hz, *J* = 2.7 Hz), 7.80 (1H, d, *J* = 2.7 Hz), 10.67 (1H, s). ¹³C NMR (DMSO-*d*₆): δ 55.95, 74.25, 105.21, 113.52, 118.45, 122.28, 124.27, 124.46, 126.83, 128.70, 129.47 (q), 131.31, 136.60, 143.88, 154.30, 177.29. MS: *m/e* 358 (MH⁺). Anal. (C₁₆H₁₁ClF₃NO₃) C, H, N.

(-)-3-(5-Chloro-2-methoxyphenyl)-1,3-dihydro-3-hydroxy-6-(trifluoromethyl)-2H-indol-2-one (**7c**). Potassium bis(trimethylsilyl)amide solution (2.2 mL, 1.1 mmol, 0.5 M in toluene) was added dropwise under an atmosphere of argon to a cold (-78 °C) stirred solution of (±)-3-(5-chloro-2-methoxyphenyl)-1,3-dihydro-6-(trifluoromethyl)-2H-indol-2-one (342 mg, 1 mmol) in dry THF (3 mL) that had been degassed by heating at reflux for 1 h while bubbling through a stream of argon. The resultant light yellow solution of the potassium enolate was stirred at -78 °C for 30 min before adding a solution of (1S)-(+)-(10-camphorsulfonyl)oxaziridine (252 mg, 1.1 mmol) in dry degassed THF (2 mL) dropwise over 5 min. The mixture was stirred at -78 °C for 1 h and then allowed to warm in an ice-bath (0–5 °C). The reaction mixture was quenched with glacial AcOH (0.1 mL), diluted with ether (25 mL) followed by addition of a saturated NH₄Cl (10 mL) solution. The organic layer was separated, washed with saturated NaHCO₃, water, and brine, and then dried (Na₂SO₄). Filtration and evaporation of the solvents gave 0.54 g of crude product, which was triturated with ether to precipitate the insoluble (camphorsulfonyl)imine byproduct, which was removed by filtration. Concentration of the filtrate gave 0.39 g of product, which was triturated with boiling CH₂Cl₂ to afford

230 mg of pure title compound. Concentration of the mother liquor followed by retrituration with CH₂Cl₂ gave an additional 72 mg of product bringing the total to 302 mg, 84% yield; mp 244–245 °C; [α]_D -132.6° (MeOH). IR (KBr, cm⁻¹): 3300–3100, 1722, 1320, 1250, 1125. ¹H NMR (DMSO-*d*₆): δ 3.42 (3H, s), 6.90 (1H, s), 6.93 (1H, d, *J* = 8.7 Hz), 7.04 (1H, d, *J* = 7.7 Hz), 7.05 (1H, s), 7.19 (1H, d, *J* = 7.7 Hz), 7.35 (1H, dd, *J* = 8.7 Hz, *J* = 2.7 Hz), 7.79 (1H, d, *J* = 2.7 Hz), 10.67 (1H, brd s). MS: *m/e* 358 (MH⁺). Anal. (C₁₆H₁₁ClF₃NO₃) C, H, N.

(+)-3-(5-Chloro-2-methoxyphenyl)-1,3-dihydro-3-hydroxy-6-(trifluoromethyl)-2H-indol-2-one (**7c**). mp 243–245 °C; [α]_D +129.9° (MeOH). IR (KBr, cm⁻¹): 3400, 1720, 1320, 1240, 1125. ¹H NMR (DMSO-*d*₆): δ 3.42 (3H, s), 6.89 (1H, s), 6.94 (1H, d, *J* = 8.7 Hz), 7.04 (1H, d, *J* = 7.7 Hz), 7.06 (1H, s), 7.20 (1H, d, *J* = 7.7 Hz), 7.36 (1H, dd, *J* = 8.6 Hz, *J* = 2.7 Hz), 7.81 (1H, d, *J* = 2.7 Hz), 10.66 (1H, s). MS: *m/e* 358 (MH⁺). Anal. (C₁₆H₁₁ClF₃NO₃) C, H, N.

(±)-3-(5-Chloro-2-methoxyphenyl)-1,3-dihydro-3-hydroxy-5-(trifluoromethyl)-2H-indol-2-one (**7d**). mp 218–220 °C. IR (KBr, cm⁻¹): 3350, 1730, 1325, 1260, 1150, 1120. ¹H NMR (DMSO-*d*₆): δ 3.41 (3H, s), 6.88 (1H, s), 6.93 (1H, d, *J* = 8.8 Hz), 7.01 (1H, d, *J* = 8.1 Hz), 7.09 (1H, d, *J* = 1.6 Hz), 7.35 (1H, dd, *J* = 8.7 Hz, *J* = 2.7 Hz), 7.56 (1H, dd, *J* = 8.1 Hz, *J* = 1.1 Hz), 7.80 (1H, d, *J* = 2.7 Hz), 10.77 (1H, s). ¹³C NMR (DMSO-*d*₆): δ 55.97, 74.26, 109.51, 113.61, 120.06, 120.11, 121.8 (m, CF₃), 124.50, 126.37, 126.94, 128.72, 131.38, 133.10, 146.70, 154.31, 177.55. MS: *m/e* 358 (MH⁺). Anal. (C₁₆H₁₁ClF₃NO₃) C, H, N.

(±)-3-(5-Chloro-2-hydroxyphenyl)-1,3-dihydro-3-hydroxy-2H-indol-2-one (**8a**). mp 216–218 °C. IR (KBr, cm⁻¹): 3520, 3328, 3204, 1700, 776, 820. ¹H NMR (DMSO-*d*₆): δ 3.39 (1H, brd s), 6.60 (1H, d, *J* = 8.5 Hz), 6.82 (3H, m), 7.14 (2H, m), 7.69 (1H, d, *J* = 2.7 Hz), 9.59 (1H, s), 10.27 (1H, s). ¹³C NMR (DMSO-*d*₆): δ 74.87, 109.13, 116.46, 121.18, 122.16, 123.71, 126.83, 127.91, 128.82, 130.19, 132.41, 143.21, 152.52, 177.67. MS: *m/e* 276 (MH⁺). Anal. (C₁₄H₁₀ClNO₃·0.4H₂O) C, H, N.

(±)-1,3-Dihydro-3-hydroxy-3-(2-hydroxyphenyl)-6-(trifluoromethyl)-2H-indol-2-one (**8b**). mp 209–211 °C (dec). ¹H NMR (DMSO-*d*₆): δ 6.59 (1H, d, *J* = 7.9 Hz), 6.62 (1H, s), 6.87 (1H, t, *J* = 7.3 Hz), 6.98 (1H, d, *J* = 7.9 Hz), 7.00 (1H, s), 7.10 (1H, m), 7.17 (1H, d, *J* = 7.5 Hz), 7.73 (1H, dd, *J* = 7.7 Hz, *J* = 1.5 Hz), 9.36 (1H, s), 10.53 (1H, s). MS: *m/e* 310 (MH⁺).

(±)-3-(5-Chloro-2-hydroxyphenyl)-1,3-dihydro-3-hydroxy-6-(trifluoromethyl)-2H-indol-2-one (**8c**). mp 210–213 °C. IR (KBr, cm⁻¹): 3300, 1725, 1320, 1250, 1170, 1140. ¹H NMR (DMSO-*d*₆): δ 6.61 (1H, dd, *J* = 8.5 Hz, *J* = 2.6 Hz), 6.81 (1H, s), 7.02, (1H, s), 7.05 (1H, d, *J* = 7.7 Hz), 7.17 (2H, m), 7.71 (1H, d, *J* = 2.7 Hz), 9.72 (1H, s), 10.60 (1H, s). ¹³C NMR (DMSO-*d*₆): δ 74.37, 105.17, 116.48, 118.30, 122.34, 124.32, 125.92, 126.84, 128.33, 129.14, 129.26 (q), 136.87, 144.11, 152.37, 177.30. MS: *m/e* 344 (MH⁺). Anal. (C₁₅H₉ClF₃NO₃) C, H, N.

(+)-3-(5-Chloro-2-hydroxyphenyl)-1,3-dihydro-3-hydroxy-6-(trifluoromethyl)-2H-indol-2-one (**8c**). Demethylation of (-)-**7c** (170 mg, 0.475 mmol) was carried out following the general procedure described in method B to provide pure titled compound (+)-**8c** (164 mg, 100%) as a white solid; mp 200–201 °C; [α]_D +119.8° (MeOH). IR (KBr, cm⁻¹): 3540, 3350, 1725, 1320, 1160, 1130. ¹H NMR (DMSO-*d*₆): δ 6.60 (1H, d, *J* = 8.5 Hz), 6.82 (1H, brd s), 7.02, (1H, s), 7.05 (1H, d, *J* = 7.6 Hz), 7.17 (2H, m), 7.71 (1H, d, *J* = 2.7 Hz), 9.75 (1H, brd s), 10.61 (1H, s). MS: *m/e* 344 (MH⁺). Anal. (C₁₅H₉ClF₃NO₃) C, H, N.

(-)-3-(5-Chloro-2-hydroxyphenyl)-1,3-dihydro-3-hydroxy-6-(trifluoromethyl)-2H-indol-2-one (**8c**). mp 198–200 °C; [α]_D -121.5° (MeOH). IR (KBr, cm⁻¹): 3540, 3300, 1725, 1320, 1125. ¹H NMR (DMSO-*d*₆): δ 6.60 (1H, d, *J* = 8.6 Hz), 6.82 (1H, brd s), 7.02, (1H, s), 7.05 (1H, d, *J* = 7.6 Hz), 7.17 (2H, m), 7.72 (1H, d, *J* = 2.7 Hz), 9.75 (1H, brd s), 10.61 (1H, s). MS: *m/e* 344 (MH⁺). Anal. (C₁₅H₉ClF₃NO₃) C, H, N.

(+)-3-(5-Chloro-2-hydroxyphenyl)-1,3-dihydro-3-hydroxy-5-(trifluoromethyl)-2H-indol-2-one (**8d**). mp 156–158 °C. IR (KBr, cm⁻¹): 3350, 1740, 1325, 1260, 1160, 1120. ¹H NMR

(DMSO-*d*₆): δ 6.62 (1H, d, J = 8.5 Hz), 6.80 (1H, s), 6.98 (1H, d, J = 8.1 Hz), 7.09 (1H, d, J = 1.2 Hz), 7.17 (1H, dd, J = 8.5 Hz, J = 2.7 Hz), 7.56 (1H, dd, J = 8.1 Hz, J = 1.2 Hz), 7.73 (1H, d, J = 2.7 Hz), 9.73 (1H, s), 10.72 (1H, s). ¹³C NMR (DMSO-*d*₆): δ 74.37, 109.44, 116.52, 120.16, 121.75 (q), 122.37, 126.42, 126.75, 126.93, 128.37, 129.28, 133.33, 146.94, 152.36, 177.56. MS: *m/e* 344 (MH⁺). Anal. (C₁₅H₉ClF₃NO₃) C, H, N.

(±)-3-(5-Chloro-2-hydroxyphenyl)-1,3-dihydro-3-hydroxy-7-(trifluoromethyl)-2H-indol-2-one (8e). mp 205–207 °C. IR (KBr, cm⁻¹): 3250, 1745, 1340, 1240, 1175, 1120. ¹H NMR (DMSO-*d*₆): δ 6.59 (1H, d, J = 8.5 Hz), 6.99 (1H, t, J = 7.7 Hz), 7.10 (1H, d, J = 7.1 Hz), 7.16 (1H, dd, J = 8.5 Hz, J = 2.7 Hz), 7.44 (1H, d, J = 7.8 Hz), 7.72 (1H, d, J = 2.7 Hz), 9.79 (1H, s), 10.79 (1H, s). ¹³C NMR (DMSO-*d*₆): δ 73.41, 110.10 (q), 116.37, 121.43, 122.27, 125.16, 125.61, 126.83, 127.53, 128.30, 129.37, 134.40, 140.72, 152.38, 178.02. MS: *m/e* 344 (MH⁺). Anal. (C₁₅H₉ClF₃NO₃·0.2H₂O) C, H, N.

(±)-3-(5-Chloro-2-hydroxyphenyl)-1,3-dihydro-3-hydroxy-4-(trifluoromethyl)-2H-indol-2-one (8f). mp 239–242 °C. IR (KBr, cm⁻¹): 3300, 1725, 1330, 1250, 1170, 1140. ¹H NMR (DMSO-*d*₆): δ 6.56 (1H, d, J = 8.5 Hz), 6.76 (1H, s), 7.07–7.13 (3H, m), 7.39 (1H, t, J = 7.9 Hz), 7.66 (1H, s), 9.57 (1H, s), 10.71 (1H, s). ¹³C NMR (DMSO-*d*₆): δ 74.93, 113.23, 116.01, 118.26, 121.60, 121.84, 125.50 (q), 127.77, 127.95, 128.76, 129.57, 129.73, 145.00, 152.40, 176.89. MS: *m/e* 344 (MH⁺). Anal. (C₁₅H₉ClF₃NO₃) C, H, N.

(±)-3-(5-Chloro-2-hydroxyphenyl)-1,3-dihydro-3-hydroxy-5-nitro-2H-indol-2-one (8g). mp 215–217 °C (dec). ¹H NMR (DMSO-*d*₆): δ 6.67 (1H, d, J = 8.5 Hz), 6.97 (1H, s), 7.02 (1H, d, J = 8.6 Hz), 7.18 (1H, dd, J = 8.5 Hz, J = 2.7 Hz), 7.62 (1H, d, J = 2.3 Hz), 7.73 (1H, d, J = 2.6 Hz), 8.17 (1H, dd, J = 8.6 Hz, J = 2.4 Hz), 9.88 (1H, s), 11.12 (1H, s). MS: *m/e* 321 (MH⁺).

(±)-3-(5-Chloro-2-hydroxyphenyl)-1,3-dihydro-3-hydroxy-5-methyl-2H-indol-2-one (8h). mp 225–227 °C (dec). IR (KBr, cm⁻¹): 3350, 1710, 1240, 820. ¹H NMR (DMSO-*d*₆): δ 2.13 (3H, s), 6.49 (1H, s), 6.60 (1H, d, J = 9.0 Hz), 6.63 (1H, d, J = 1.0 Hz), 6.67 (1H, d, J = 7.8 Hz), 6.94 (1H, dd, J = 7.75 Hz, J = 1.0 Hz), 7.12 (1H, dd, J = 8.5 Hz, J = 2.8 Hz), 7.68 (1H, d, J = 2.7 Hz), 9.57 (1H, s), 10.17 (1H, s). MS: *m/e* 290 (MH⁺). Anal. (C₁₅H₁₂ClNO₃) C, H, N.

(±)-3-(5-Chloro-2-hydroxyphenyl)-1,3-dihydro-5-fluoro-3-hydroxy-2H-indol-2-one (8i). mp 158–161 °C (dec). IR (KBr, cm⁻¹): 3300, 1710, 1250. ¹H NMR (DMSO-*d*₆): δ 3.36 (1H, brd s), 6.61 (1H, d, J = 8.5 Hz), 6.68 (1H, dd, J = 8.0 Hz, J = 2.6 Hz), 6.77 (1H, dd, J = 8.5 Hz, J = 4.3 Hz), 6.98 (1H, ddd, J = 8.5 Hz, J = 8.0 Hz, J' = 2.6 Hz), 7.15 (1H, dd, J = 8.5 Hz, J = 2.7 Hz), 7.68 (1H, d, J = 2.7 Hz), 9.65 (1H, s), 10.32 (1H, s). MS: *m/e* 294 (MH⁺).

(±)-3-(5-Chloro-2-hydroxyphenyl)-4,6-dichloro-1,3-dihydro-3-hydroxy-2H-indol-2-one (8j). mp 232–235 °C (dec). IR (KBr, cm⁻¹): 3400, 1730, 1275. ¹H NMR (DMSO-*d*₆): δ 6.61 (1H, d, J = 8.5 Hz), 6.79 (1H, d, J = 1.7 Hz), 6.81 (1H, s), 6.94 (1H, d, J = 1.7 Hz), 7.14 (1H, dd, J = 8.5 Hz, J = 2.7 Hz), 7.71 (1H, d, J = 2.7 Hz), 9.71 (1H, s), 10.71 (1H, s). ¹³C NMR (DMSO-*d*₆): δ 74.77, 108.31, 116.32, 121.22, 122.07, 127.55, 128.20, 128.39, 130.40, 134.05, 146.26, 152.27, 176.89. MS: *m/e* 344 (MH⁺). Anal. (C₁₄H₈Cl₂NO₃) C, H, N.

(±)-3-(5-Chloro-2-hydroxyphenyl)-1,3-dihydro-3-hydroxy-4,6-bis(trifluoromethyl)-2H-indol-2-one (8k). mp 191–193 °C. IR (KBr, cm⁻¹): 3700–2500, 1740, 1280, 1170, 1130. ¹H NMR (DMSO-*d*₆): δ 6.59 (1H, d, J = 8.5 Hz), 7.06 (1H, s), 7.15 (1H, dd, J = 8.5 Hz, J = 2.6 Hz), 7.34 (1H, s), 7.45 (1H, s), 7.68 (1H, d, J = 2.6 Hz), 9.74 (1H, s), 11.07 (1H, s). MS: *m/e* 412 (MH⁺). Anal. (C₁₆H₈ClF₆NO₃·0.2H₂O) C, H, N.

(±)-1,3-Dihydro-3-(5-fluoro-2-hydroxyphenyl)-3-hydroxy-6-(trifluoromethyl)-2H-indol-2-one (8l). mp 184–186 °C. ¹H NMR (DMSO-*d*₆): δ 6.57 (1H, dd, J = 8.8, J = 4.7 Hz), 6.78 (1H, brd s), 6.94 (1H, ddd, J = 8.5 Hz, J = 8.5 Hz, J' = 3.2 Hz), 7.01 (1H, s), 7.03 (1H, d, J = 7.7 Hz), 7.18 (1H, d, J = 7.7 Hz), 7.49 (1H, dd, J = 10.0 Hz, J = 3.2 Hz), 9.41 (1H, s), 10.59 (1H, s). MS: *m/e* 328 (MH⁺). Anal. (C₁₅H₉F₄NO₃) H, N; C: calcd, 55.06; found, 54.69.

(±)-3-(5-Bromo-2-hydroxyphenyl)-1,3-dihydro-3-hydroxy-6-(trifluoromethyl)-2H-indol-2-one (8m). mp 194–196 °C. ¹H NMR (DMSO-*d*₆): δ 6.56 (1H, d, J = 8.5 Hz), 6.82 (1H, brd s), 7.02 (1H, s), 7.05 (1H, d, J = 7.7 Hz), 7.19 (1H, dd, J = 7.7 Hz, J = 0.6 Hz), 7.28 (1H, dd, J = 8.5 Hz, J = 2.6 Hz), 7.84 (1H, d, J = 2.6 Hz), 9.77 (1H, s), 10.62 (1H, s). MS: *m/e* 390 (MH⁺).

(±)-1,3-Dihydro-3-hydroxy-3-(5-iodo-2-hydroxyphenyl)-6-(trifluoromethyl)-2H-indol-2-one (8n). mp 192–194 °C. ¹H NMR (DMSO-*d*₆): δ 6.45 (1H, d, J = 8.4 Hz), 6.78 (1H, s), 7.01 (1H, s), 7.04 (1H, d, J = 7.6 Hz), 7.18 (1H, d, J = 7.6 Hz), 7.43 (1H, dd, J = 8.4 Hz, J = 2.3 Hz), 8.01 (1H, d, J = 2.3 Hz), 9.74 (1H, s), 10.59 (1H, s). MS: *m/e* 436 (MH⁺). Anal. (C₁₅H₉F₃INO₃) C, H, N.

(±)-1,3-Dihydro-3-hydroxy-3-(2-hydroxy-5-methylphenyl)-6-(trifluoromethyl)-2H-indol-2-one (8o). mp 226–228 °C (dec). ¹H NMR (DMSO-*d*₆): δ 2.26 (3H, s), 6.47 (1H, s, J = 8.1 Hz), 6.59 (1H, s), 6.90 (1H, dd, J = 8.1 Hz, J = 2.0 Hz), 6.98–7.01 (2H, m), 7.17 (1H, d, J = 7.7 Hz), 7.55 (1H, d, J = 2.0 Hz), 9.11 (1H, s), 10.51 (1H, s). MS: *m/e* 324 (MH⁺). Anal. (C₁₆H₁₂F₃NO₃) C, H, N.

(±)-1,3-Dihydro-3-hydroxy-3-(4-hydroxy-1,1'-biphenyl-3-yl)-6-(trifluoromethyl)-2H-indol-2-one (8p). mp 180–185 °C (dec). ¹H NMR (DMSO-*d*₆): δ 6.67 (1H, d, J = 8.3 Hz), 7.03 (1H, s), 7.08 (1H, d, J = 7.7 Hz), 7.19 (1H, d, J = 7.7 Hz), 7.29 (2H, t, J = 7.3 Hz), 7.40–7.48 (3H, m), 7.62 (2H, d, J = 7.3 Hz), 8.04 (1H, d, J = 1.9 Hz), 9.60 (1H, brd s), 10.58 (1H, s). MS: *m/e* 386 (MH⁺). Anal. (C₂₁H₁₄F₃NO₃) C, H, N.

(±)-1,3-Dihydro-3-hydroxy-3-(2-hydroxy-1-naphthalenyl)-6-(trifluoromethyl)-2H-indol-2-one (8q). mp 159–160 °C. ¹H NMR (DMSO-*d*₆): δ 6.96 (1H, d, J = 8.4 Hz), 7.06 (1H, s), 7.16 (1H, d, J = 7.8 Hz), 7.22–7.31 (3H, m), 7.42 (1H, brd s), 7.71 (1H, d, J = 8.7 Hz), 7.78 (1H, d, J = 8.0 Hz), 9.35 (1H, brd s), 9.99 (1H, brd s), 10.48 (1H, brd s). MS: *m/e* 358 (M – H)⁻. Anal. (C₁₉H₁₂F₃NO₃·0.85H₂O) C, H, N.

(±)-3-(4-Amino-2-hydroxyphenyl)-1,3-dihydro-3-hydroxy-6-(trifluoromethyl)-2H-indol-2-one (8r). mp 276–280 °C (dec). ¹H NMR (DMSO-*d*₆): δ 4.92 (2H, s), 5.88 (1H, d, J = 1.9 Hz), 6.06 (1H, dd, J = 8.3, J = 1.9 Hz), 6.35 (1H, s), 6.98 (1H, s), 7.01 (1H, d, J = 7.7 Hz), 7.17 (1H, d, J = 7.7 Hz), 7.27 (1H, d, J = 8.3 Hz), 8.86 (1H, s), 10.42 (1H, s). MS: *m/e* 325 (MH⁺).

(±)-1,3-Dihydro-3-hydroxy-3-(2-hydroxy-5-methoxyphenyl)-6-(trifluoromethyl)-2H-indol-2-one (8s). mp 231–233 °C. ¹H NMR (DMSO-*d*₆): δ 3.72 (3H, s), 6.50 (1H, d, J = 8.6 Hz), 6.65 (1H, s), 6.69 (1H, dd, J = 8.6 Hz, J = 3.1 Hz), 7.02 (1H, d, J = 7.5 Hz), 7.00 (1H, s), 7.17 (1H, d, J = 7.5 Hz), 7.33 (1H, d, J = 3.1 Hz), 8.90 (1H, s), 10.53 (1H, s). MS: *m/e* 340 (MH⁺). Anal. (C₁₆H₁₂F₃NO₄) C, H, N.

(±)-1,3-Dihydro-3-hydroxy-3-[2-hydroxy-5-(4-methylpiperazin-1-yl)phenyl]-6-(trifluoromethyl)-2H-indol-2-one (8t). mp 210–215 °C (dec). IR (KBr, cm⁻¹): 3350, 1735, 1320, 1250, 1170, 1125. ¹H NMR (DMSO-*d*₆): δ 2.26 (3H, s), 2.52 (4H, m), 3.04 (4H, m), 3.32 (3H, s), 6.47 (1H, d, J = 8.6 Hz), 6.58 (1H, s), 6.71 (1H, dd, J = 8.6 Hz, J = 2.9 Hz), 6.99 (1H, s), 7.01 (1H, d, J = 8.3 Hz), 7.16 (1H, d, J = 8.3 Hz), 7.38 (1H, d, J = 2.9 Hz), 8.81 (1H, s), 10.49 (1H, s). MS: *m/e* 408 (MH⁺).

(±)-1,3-Dihydro-3-hydroxy-3-[2-hydroxy-5-(trifluoromethyl)phenyl]-6-(trifluoromethyl)-2H-indol-2-one (8u). mp 175–177 °C. ¹H NMR (DMSO-*d*₆): δ 6.77 (1H, d, J = 8.3 Hz), 7.02–7.09 (3H, m), 7.19 (1H, d, J = 7.7 Hz), 7.51 (1H, d, J = 8.3 Hz), 8.08 (1H, s), 10.40 (1H, s), 10.67 (1H, s). MS: *m/e* 378 (MH⁺). Anal. (C₁₆H₉F₆NO₃) C, H, N.

(±)-1,3-Dihydro-3-hydroxy-3-[2-hydroxy-4-(trifluoromethyl)phenyl]-6-(trifluoromethyl)-2H-indol-2-one (8v). mp 198–201 °C. ¹H NMR (DMSO-*d*₆): δ 6.97 (1H, s), 7.01–7.06 (3H, m), 7.11 (1H, dd, J = 8.7 Hz, J = 2.5 Hz), 7.23 (1H, d, J = 7.7 Hz), 7.99 (1H, d, J = 8.7 Hz), 10.18 (1H, s), 10.67 (1H, s). MS: *m/e* 378 (MH⁺). Anal. (C₁₆H₉F₆NO₃·0.7H₂O) C, H, N.

(±)-3-(3-Chloro-2-hydroxyphenyl)-1,3-dihydro-3-hydroxy-6-(trifluoromethyl)-2H-indol-2-one (8w). mp 202–205 °C. ¹H NMR (DMSO-*d*₆): δ 6.77 (1H, s), 6.90 (1H, t, J = 7.8 Hz), 7.04 (1H, s), 7.02 (1H, d, J = 7.8 Hz), 7.21 (1H, d, J = 7.8

Hz), 7.30 (1H, dd, $J = 8.0$ Hz, $J = 1.6$ Hz), 7.69 (1 H, dd, $J = 8.0$ Hz, $J = 1.0$ Hz), 9.46 (1H, s), 10.68 (1H, s). MS: m/e 344 (MH⁺).

(±)-3-(4-Chloro-2-hydroxyphenyl)-1,3-dihydro-3-hydroxy-6-(trifluoromethyl)-2H-indol-2-one (**8x**). mp 188–190 °C (dec). ¹H NMR (DMSO-*d*₆): δ 6.64 (1H, d, $J = 2.0$ Hz), 6.75 (1H, s), 6.95 (1H, dd, $J = 8.3$ Hz, $J = 2.0$ Hz), 7.00 (1H, d, $J = 8.3$ Hz), 7.02 (1H, s), 7.19 (1H, d, $J = 8.3$ Hz), 7.75 (1H, d, $J = 8.3$ Hz), 9.96 (1H, s), 10.59 (1H, s). MS: m/e 344 (MH⁺).

(±)-3-(4,5-Dichloro-2-hydroxyphenyl)-1,3-dihydro-3-hydroxy-6-(trifluoromethyl)-2H-indol-2-one (**8y**). mp 152–154 °C. ¹H NMR (CDCl₃/DMSO-*d*₆): δ 5.22 (1H, s), 6.83 (1H, s) 7.04 (1H, s), 7.14 (1H, d, $J = 7.8$ Hz), 7.20 (1H, d, $J = 7.8$ Hz), 7.32 (1H, s), 9.50 (1H, brd s), 9.96 (1H, brd s). MS: m/e 378 (MH⁺).

(±)-3-(3,5-Dichloro-2-hydroxyphenyl)-1,3-dihydro-3-hydroxy-6-(trifluoromethyl)-2H-indol-2-one (**8z**). mp 210–212 °C. ¹H NMR (DMSO-*d*₆): δ 6.19 (1H, brd s), 6.91 (1H, s), 6.97 (1H, s), 7.21 (1H, d, $J = 7.8$ Hz), 7.43 (1H, d, $J = 7.7$ Hz), 9.25 (1H, s), 10.38 (1H, s). MS: m/e 376 (M – H).

(±)-3-(4-Amino-5-chloro-2-hydroxyphenyl)-1,3-dihydro-3-hydroxy-6-(trifluoromethyl)-2H-indol-2-one (**8za**). mp 198–200 °C. ¹H NMR (DMSO-*d*₆): δ 5.18 (2H, s), 6.09 (1H, s), 6.50 (1H, s), 6.98 (1H, s), 7.05 (1H, d, $J = 7.6$ Hz), 7.18 (1H, d, $J = 7.2$ Hz), 7.44 (1H, s), 9.15 (1H, s), 10.45 (1H, s). MS: m/e 359 (MH⁺). Anal. (C₁₅H₁₀ClF₃N₂O₃) C, H, N: calcd, 7.81; found, 7.33.

(±)-3-(5-Chloro-3-iodo-2-hydroxyphenyl)-1,3-dihydro-3-hydroxy-6-(trifluoromethyl)-2H-indol-2-one (**8zb**). A solution of iodine monochloride (104 mg, 0.64 mmol) in glacial AcOH (10 mL) was added to a cold (5–10 °C) stirred solution of **8c** (200 mg, 0.58 mmol) in AcOH (20 mL) maintained under an atmosphere of nitrogen. The mixture was allowed to warm to room temperature and stirred overnight before it was poured into cold water and extracted with ether. The ether extract was washed with 10% NaHSO₃ solution, water, and brine and then dried over Na₂SO₄. Filtration followed by concentration in a vacuum gave a brown solid (0.25 g), which was triturated with warm CH₂Cl₂ to afford pure iodinated phenol **8zb**; mp 210–212 °C (dec). IR (KBr, cm⁻¹): 3600–2500, 1730, 1320, 1170, 1140. ¹H NMR (DMSO-*d*₆): δ 7.06 (1H, s), 7.09 (1H, s), 7.12 (1H, d, $J = 7.8$ Hz), 7.25 (1H, d, $J = 7.8$ Hz), 7.69 (1H, d, $J = 2.6$ Hz), 7.75 (1H, d, $J = 2.6$ Hz), 9.25 (1H, s), 10.70 (1H, s). MS: m/e 470 (MH⁺). Anal. (C₁₅H₈ClF₃INO₃) C, H, N.

(±)-3-(5-Chloro-2-methoxyphenyl)-1,3-dihydro-6-(trifluoromethyl)-2H-indol-2-one (**10b**). mp 210–213 °C. IR (KBr, cm⁻¹): 3200, 1710, 1320, 1250, 1170, 1120, 1050. ¹H NMR (DMSO-*d*₆): δ 3.57 (3H, s), 4.91 (1H, s) 7.02 (1H, d, $J = 8.8$ Hz), 7.06 (2H, m), 7.21, (1H, dd, $J = 7.7$ Hz, $J = 0.6$ Hz), 7.35 (2H, m), 10.77 (1H, s). ¹³C NMR (DMSO-*d*₆): δ 48.25, 56.07, 105.05, 113.58, 118.26, 122.42, 124.18, 126.03, 127.38, 128.60 (q), 128.70, 130.65, 134.37, 143.58, 156.09, 176.73. MS: m/e 342 (MH⁺). Anal. (C₁₆H₁₁ClF₃NO₂) C, H, N.

(±)-3-(5-Chloro-2-hydroxyphenyl)-1,3-dihydro-2H-indol-2-one (**11a**). mp 256–258 °C. IR (KBr, cm⁻¹): 3300, 3200, 1680, 820, 750. ¹H NMR (DMSO-*d*₆): δ 4.75 (1H, s), 6.78 (1H, d, $J = 8.6$ Hz), 6.85 (2H, t, $J = 8.1$ Hz), 6.92 (1H, d, $J = 7.2$ Hz), 7.08 (1H, d, $J = 2.5$ Hz), 7.11–7.17 (2H, m), 8.78 (1H, s), 10.46 (1H, s). ¹³C NMR (DMSO-*d*₆): δ 48.04, 109.09, 116.87, 121.31, 122.20, 123.72, 126.61, 127.64, 127.99, 130.01, 130.05, 142.78, 154.40, 177.17. MS: m/e 260 (MH⁺). Anal. (C₁₄H₁₀ClNO₂) C, H, N.

(±)-3-(5-Chloro-2-hydroxyphenyl)-1,3-dihydro-6-(trifluoromethyl)-2H-indol-2-one (**11b**). Demethylation of **10b** (1.37 g, 4 mmol) was carried out following the general procedure described in method B to afford **11b** (1.21 g, 93%) as an off-white solid; mp 266–268 °C. IR (KBr, cm⁻¹): 3320, 1690, 1310, 1250, 1160, 1125. ¹H NMR (DMSO-*d*₆): δ 4.85 (1H, s), 6.75 (1H, d, $J = 8.6$ Hz), 7.04 (1H, s), 7.11, (1H, d, $J = 7.7$ Hz), 7.17 (1H, dd, $J = 8.6$ Hz, $J = 2.6$ Hz), 7.22 (1H, d, $J = 8.0$ Hz), 7.26 (1H, d, $J = 2.4$ Hz), 9.82 (1H, s), 10.73 (1H, s). ¹³C NMR (DMSO-*d*₆): δ 48.47, 104.94, 116.84, 118.16, 122.27,

124.20, 125.61, 126.06, 128.05, 128.41, 130.76, 134.72, 143.69, 154.26, 176.92. MS: m/e 328 (MH⁺). Anal. (C₁₅H₉ClF₃NO₂) C, H, N.

In Vitro and In Vivo Methods. Recording of Whole Cell Maxi-K (*mSlo* or *hSlo*)-Mediated Outward Currents Expressed in *Xenopus* Oocytes. The ability of compounds listed in Table 1 to open maxi-K channels and increase whole cell outward (K⁺) maxi-K-mediated currents was assessed under voltage clamp conditions by determining their ability to increase cloned mammalian (*mSlo* or *hSlo*) maxi-K-mediated outward current heterologously expressed in *Xenopus* oocytes.^{37,38} The two maxi-K constructs employed represent nearly structurally identical homologous proteins and have proven to be pharmacologically identical in our tests. To isolate maxi-K current from native (background, nonmaxi-K) current, the specific and potent maxi-K channel-blocking toxin, IbTX,⁴⁴ was employed at a supramaximal concentration (50 nM). The relative contribution of maxi-K channels current to total outward current was determined by subtraction of the current remaining in the presence of IbTX (nonmaxi-K current) from the current profiles obtained in all other experimental conditions (control, drug, and wash).³⁹ It was determined that at the tested concentration the compounds profiled did not affect nonmaxi-K native currents in the oocytes.³⁹ All compounds were tested in at least five oocytes and are reported at the single concentration of 20 μ M; the effect of compounds on maxi-K current was expressed as the percent of control IbTX-sensitive current, and it is listed in Table 1. Recordings were accomplished using standard two electrode voltage clamp techniques;⁴⁵ voltage clamp protocols consisted of 500–750 ms duration step depolarizations from a holding potential of –60 to +140 mV in 20 mV steps. The experimental media (modified Barth's solution) consisted of (in mM) NaCl (88), NaHCO₃ (2.4), KCl (1.0), HEPES (10), MgSO₄ (0.82), Ca(NO₃)₂ (0.33), and CaCl₂ (0.41); pH 7.5.

Pharmacokinetic Studies. For evaluation of brain uptake, (±)-**8c** and (±)-**11b** were each dissolved (10% DMSO/65% poly(ethylene glycol)/25% water; 2.5 mg/mL), and 2 mL/kg of each solution was administered as a bolus via the tail vein to male Sprague–Dawley rats (ca. 225 g). Three animals from each group were killed (CO₂ inhalation) at 0.25 and 2 h, the whole brain was removed, and a blood sample was obtained. Aqueous whole brain homogenates and plasma samples were extracted with CH₃CN and analyzed by a high-performance liquid chromatography assay with UV (290 nm) detection. For the pharmacokinetic evaluation of (±)-**8c** in rats, 24 male rats were dosed as above, with three animals killed at intervals out to 8 h after dosing. Brains and blood samples were removed and analyzed for (±)-**8c**. For metabolite identification, (±)-**8c** and (±)-**11b** were separately incubated at a final concentration of 25 μ g/mL in a freshly prepared rat liver 9000 g supernatant fraction (S9) fortified with cofactors (NADPH, MgCl₂, glucose-6-phosphate, and glucose-6-phosphate dehydrogenase) for 1 h.⁵⁰ Over time, aliquots of each incubation mixture were removed, extracted with CH₃CN, and analyzed for (±)-**8c** or (±)-**11b**. Metabolite identification (LC/MS/MS: Sciex API III tandem quadrupole) was conducted on samples following the 1 h incubation.

MCAO Protocol. Male SHR (from Taconic Farms, Inc. or Harlan), weighing 240–350 gm, were anesthetized with a combination of ketamine (40 mg/kg, i.m.) and xylazine (4.5 mg/kg). According to the method described by Tamura et al.,⁴⁶ a subtemporal approach was used to occlude the left MCA. Prior to making the initial incision, 0.2 mg of xylocaine was injected into the scalp. Muscle tissue covering the rostral end of the zygoma at its fusion to the squamosal bone was excised. With a no. 6 dental burr, a craniotomy was performed to locate the MCA. A 2 mm segment of the MCA, containing the origins of the lenticulostriate arteries, was electrocauterized with bipolar forceps, and then, the cauterized artery was severed to ensure permanent occlusion. Sterile Gelfoam was placed in the wound that was then sutured. Colonic and temporalis temperatures were recorded immediately prior to surgery, at the time of occlusion, and 1 h postocclusion. Body temperature was

monitored during the procedure and maintained between 36 and 38 °C through the use of a heating pad. Experimental compounds or vehicle alone were administered via tail vein injection or intraperitoneally. The vehicle solution for experimental compounds was 2% DMSO and 98% propylene glycol. Twenty-four hours after occlusion, the rats were administered an overdose of methoxyflurane anesthesia. A 3% solution of the vital dye 2,3,5-triphenyltetrazolium chloride (10 mL) was infused through the thoracic aorta. The brains were quickly removed and incubated in the vital dye for 30 min at 37 °C and then placed in buffered 10% formalin for 3–5 days. Coronal slices, 2 mm thickness, were prepared, and infarct volume was quantified using computer-assisted planimetry.⁴⁷

[³H]-Glutamate Release. Hippocampal tissue (350 μm wedges) from male Sprague–Dawley rats was washed 5× in Krebs's buffer containing (mM) NaCl (125), KCl (3.0), MgSO₄ (1.2), CaCl₂ (1.2), NaHCO₃ (22), NaH₂PO₄ (10), glucose (10), and 1 unit of adenosine deaminase/mL. Tissue was incubated at 37 °C for 30 min in buffer containing 5 μCi of [³H]-glutamate (New England Nuclear; specific activity = 50–60 Ci/mM). Tissue was transferred to superfusion chambers (Brandel Instruments) and washed with buffer for 60 min at a flow rate of 1 mL/min. The wash buffer was discarded, and 5 min fractions were collected thereafter at a flow rate of 0.5 mL/min. Release of [³H]-glutamate was evoked by field electrical stimulation (35 mA, 10 Hz, pulse width 2 ms, duration 1 min). Tissue was stimulated for the first minute of fractions 3 (S₁) and 13 (S₂). Test compound (**8c** or **11b**) was introduced 30 min prior to S₂ (fraction 7) and removed at the end of fraction 15. Radioactivity was quantified using liquid scintillation spectroscopy, and data were expressed as the ratio S₂/S₁ over a range of concentrations. Statistical analysis consisted of analysis of variance (ANOVA) followed by post-hoc testing (Newmann–Keuls).

Supporting Information Available: Single crystal X-ray crystallographic data for (3*R*)-(-)-5-bromo-3-(5-chloro-2-methoxyphenyl)-1,3-dihydro-3-hydroxy-2*H*-indol-2-one. This material is available free of charge via the Internet at <http://pubs.acs.org>.

References

- Williams, G. R.; Jiang, J. G.; Matchar, D. B.; Samsa, G. P. Incidence and Occurrence of Total (First-ever and Recurrent) Stroke. *Stroke* **1999**, *30*, 2523–2528.
- Fisher, M. Antithrombotic and Thrombolytic Therapy for Ischemic Stroke. *J. Thromb. Thrombolysis* **1999**, *7*, 165–169.
- Pellegrini-Giampietro, D. E.; Pulsinelli, W. A.; Zukin, R. S. NMDA and Non-NMDA Receptor Gene Expression Following Global Brain Ischemia in Rats: Effect of NMDA and Non-NMDA Receptor Antagonists. *J. Neurochem.* **1994**, *62*, 1067–1073.
- Wilding, T. J.; Huettner, J. E. Antagonist Pharmacology of Kainate- and Alpha-amino-3-hydroxy-5-methyl-4-isoxazolepropionic Acid-Preferring Receptors. *Mol. Pharmacol.* **1996**, *49*, 540–546.
- Goldberg, M. P.; Strasser, U.; Dugan, L. L. Techniques for Assessing Neuroprotective Drugs In Vitro. *Int. Rev. Neurobiol.* **1997**, *40*, 69–93.
- Gagliardi, R. J. Neuroprotection, Excitotoxicity and NMDA Antagonists. *Arq. Neuro-Psiquiatr.* **2000**, *58*, 583–588.
- Miller, L. P.; Hsu, C. Therapeutic Potential for Adenosine Receptor Activation in Ischemic Brain Injury. *J. Neurotrauma* **1992**, *9*, 563–577.
- Sweeney, M. I. Neuroprotective Effects of Adenosine in Cerebral Ischemia: Window of Opportunity. *Neurosci. Biobehav. Rev.* **1997**, *21*, 207–217.
- De Keyser, J.; Sulter, G.; Luiten, P. G. Clinical Trials with Neuroprotective Drugs in Acute Ischaemic Stroke: Are We Doing the Right Thing? *Trends Neurosci.* **1999**, *22*, 535–540.
- Choi, D. W. Calcium: Still Center-stage in Hypoxic-Ischemic Neuronal Death. *Trends Neurosci.* **1995**, *18*, 58–60.
- Kristian, T.; Siesjö, B. K. Calcium in Ischemic Cell Death. *Stroke* **1998**, *29*, 705–718.
- Choi, D. W. Excitotoxic Cell Death. *J. Neurobiol.* **1992**, *23*, 1261–1276.
- Dirnagl, U.; Iadecola, C.; Moskowitz, M. A. Pathobiology of Ischaemic Stroke: An Integrated View. *Trends Neurosci.* **1999**, *22*, 391–397.
- Cook, N. S. The Pharmacology of Potassium Channels and Their Therapeutic Potential. *Trends Pharmacol. Sci.* **1988**, *9*, 21–28.
- Quast, U.; Cook, N. S. Moving Together: K⁺ Channel Openers and ATP-Sensitive K⁺ Channels. *Trends Pharmacol. Sci.* **1989**, *10*, 431–435.
- Longman, S. D.; Hamilton, T. C. Potassium Channel Activator Drugs: Mechanism of Action, Pharmacological Properties, and Therapeutic Potential. *Med. Res. Rev.* **1992**, *12*, 73–148.
- Atwal, K. S. Modulation of Potassium Channels by Organic Molecules. *Med. Res. Rev.* **1992**, *12*, 569–591.
- Gopalakrishnan, M.; Janis, R. A.; Triggle, D. J. ATP-Sensitive K⁺ Channels: Pharmacologic Properties, Regulation, and Therapeutic Potential. *Drug Dev. Res.* **1993**, *28*, 95–127.
- Shieh, C. C.; Coghlan, M.; Sullivan, J. P.; Gopalakrishnan, M. Potassium Channels: Molecular Defects, Diseases, and Therapeutic Opportunities. *Pharmacol. Rev.* **2000**, *52*, 557–594.
- LaTorre, R.; Oberhauser, A.; Labarca, P.; Alvarez, O. Varieties of Calcium-Activated Potassium Channels. *Annu. Rev. Physiol.* **1989**, *51*, 385–399.
- Sah, P. Ca²⁺-Activated K⁺ Currents in Neurons: Types, Physiological Roles and Modulation. *Trends Neurosci.* **1996**, *19*, 150–154.
- Starrett, J. E.; Dworetzky, S. I.; Gribkoff, V. K. Modulators of Large-conductance Calcium-activated Potassium (BK) Channels as Potential Therapeutic Targets. *Curr. Pharm. Des.* **1996**, *2*, 413–428.
- Gribkoff, V. K.; Starrett, J. E.; Dworetzky, S. I. The Pharmacology and Molecular Biology of Large-conductance Calcium-activated (BK) Potassium Channels. *Adv. Pharmacol.* **1997**, *37*, 319–348.
- Olesen, S.-P. Activators of Large Conductance, Ca²⁺-Dependent K⁺ Channels. *Exp. Opin. Invest. Drugs* **1994**, *3*, 1181–1188.
- Olesen, S.-P.; Munch, E.; Moldt, P.; Drejer, J. Selective Activation of Ca²⁺-Dependent K⁺ Channels by Novel Benzimidazolone. *Eur. J. Pharmacol.* **1994**, *251*, 53–59.
- Olesen, S.-P.; Munch, E.; Wätjen, F.; Drejer, J. NS 004-an Activator of Ca²⁺-Dependent K⁺ Channels in Cerebellar Granule Cells. *NeuroReport* **1994**, *5*, 1001–1004.
- McKay, M. C.; Dworetzky, S. I.; Meanwell, N. A.; Olesen, S.-P.; Reinhart, P. H.; Levitan, I. B.; Adelman, J. P.; Gribkoff, V. K. Opening of Large-Conductance Calcium-Activated Potassium Channels by the Substituted Benzimidazolone NS004. *J. Neurophysiol.* **1994**, *71*, 1873–1882.
- Xu, X.; Tsai, T. D.; Wang, J.; Lee, E. W.; Lee, K. S. Modulation of Three Types of K⁺ Currents in Canine Coronary Artery Smooth Muscle Cells by NS-004, or 1-(2'-hydroxy-5'-chlorophenyl)-5-trifluoromethyl-2(3*H*)-benzimidazolone. *J. Pharmacol. Exp. Ther.* **1994**, *271*, 362–369.
- Edwards, G.; Niederste-Hollenberg, A.; Schneider, J.; Noack, T.; Weston, A. H. Ion Channel Modulation by NS 1619, the Putative BKCa Channel Opener, in Vascular Smooth Muscle. *Br. J. Pharmacol.* **1994**, *113*, 1538–1547.
- Lee, K.; Rowe, I. C.; Ashford, M. L. NS 1619 Activates BKCa Channel Activity in Rat Cortical Neurons. *Eur. J. Pharmacol.* **1995**, *280*, 215–219.
- Meanwell, N. A.; Sit, S.-Y.; Gao, J.; Boissard, C. G.; Lum-Ragan, J.; Dworetzky, S. I.; Gribkoff, V. K. N-Benzylated Benzimidazol-2-one Derivatives: Activators of Large-Conductance Ca²⁺-Dependent K⁺ Channels. *Bioorg. Med. Chem. Lett.* **1996**, *6*, 1641–1646.
- Hewawasam, P.; Meanwell, N. A.; Gribkoff, V. K.; Dworetzky, S. I.; Boissard, C. G. Discovery of a Novel Class of BK Channel Openers: Enantiospecific Synthesis and BK Channel Opening Activity of 3-(5-Chloro-2-hydroxyphenyl)-1,3-dihydro-3-hydroxy-6-(trifluoromethyl)-2*H*-indol-2-one. *Bioorg. Med. Chem. Lett.* **1997**, *7*, 1255–1260.
- Hewawasam, P.; Meanwell, N. A. A General Method for the Synthesis of Isatins: Preparation of Regiospecifically Functionalized Isatins from Anilines. *Tetrahedron Lett.* **1994**, *35*, 7303–7306.
- Hewawasam, P.; Erway, M. Reactivity and Regioselectivity of Magnesium Phenolates towards Isatins: One-step Synthesis of 3-(2-Hydroxyaryl)-3-hydroxyindolones. *Tetrahedron Lett.* **1998**, *39*, 3981–3984.
- Davis, F. A.; Chen, B.-C. Asymmetric Hydroxylation of Enolates with N-Sulfonyloxaziridines. *Chem. Rev.* **1992**, *92*, 919–934.
- Previously, chiral shift reagents have been used to determine the enantiomeric excess of chiral alcohols as described in ref 35. However, for this series of chiral alcohols, we have found that chiral solvent (L)-trifluoromethylphenyl carbinol can be used in place of chiral shift reagents to effectively determine the enantiomeric excess of **7c** and **8c**.
- Butler, A.; Tsunoda, S.; McCobb, D. P.; Wei, A.; Salkoff, L. *mSlo*, a Complex Mouse Gene Encoding “Maxi” Calcium-Activated Potassium Channels. *Science* **1993**, *261*, 221–224.
- Dworetzky, S. I.; Trojnacki, J. T.; Gribkoff, V. K. Cloning and Expression of a Human Large-Conductance Calcium-Activated Potassium Channel. *Mol. Brain Res.* **1994**, *27*, 189–193.

- (39) Gribkoff, V. K.; Lum-Ragan, J. T.; Boissard, C. G.; Post-Munson, D. J.; Meanwell, N. A.; Starrett, J. E., Jr.; Kozlowski, E. S.; Romine, J. L.; Trojnacki, J. T.; McKay, M. C.; Zhong, J.; Dworetzky, S. I. Effects of Channel Modulators on Cloned Large-Conductance Calcium-Activated Potassium Channels. *Mol. Pharmacol.* **1996**, *50*, 206–217.
- (40) Lees, K. R. Cerestat and other NMDA Antagonists in Ischemic Stroke. *Neurology* **1997**, *49*, 66–69.
- (41) Diener, H. C.; Cortens, M.; Ford, G.; Grotta, J.; Hacke, W.; Kaste, M.; Koudstaal, P. J.; Wessel, T. Lubeluzole in Acute Ischemic Stroke Treatment: A Double-Blind Study with an 8-Hour Inclusion Window Comparing a 10-mg Daily Dose of Lubeluzole with Placebo. *Stroke* **2000**, *31*, 2543–2551.
- (42) This general trend has been established with a variety of chemically distinct maxi-K openers that have been identified from our yet unpublished work.
- (43) Hewawasam, P.; Dworetzky, S. I.; Ortiz, A. A.; Kinney, G. G.; Boissard, C. G.; Post-Munson, D. J.; Trojnacki, J. T.; Huston, K.; Signor, L. J.; Lombardo, L. A.; Reid, S. A.; Hibbard, J. R.; Myers, R. A.; Moon, S. L.; Weiner, H. L.; Thalody, G.; Yeleswaram, K.; Pajor, L. M.; Knipe, J. O.; Meanwell, N. A.; Johnson, G.; Molinoff, P. B.; Starrett, J. E.; Gao, Q. Discovery of Openers of Large-Conductance, Calcium-Activated Potassium (Maxi-K) Channels: A New Approach to Stroke Neuroprotection; *Proceedings of the 219th American Chemical Society National Meeting*, San Francisco, CA, March 26–30, 2000; MEDI 320.
- (44) Galvez, A.; Gimenez-Gallego, G.; Reuben, J. P.; Roy-Contancin, L.; Feigenbaum, P.; Kaczorowski, G. J.; Garcia, M. L. Protein Purification and characterization of a unique, potent, peptidyl probe for the high conductance calcium-activated potassium channel from venom of the scorpion *Buthus tamulus*. *J. Biol. Chem.* **1990**, *265*, 11083–11090.
- (45) Stuhmer, W. Electrophysiological recording from *Xenopus* oocytes. *Methods Enzymol.* **1992**, *207*, 319–339.
- (46) Tamura, A.; Kirino, T.; Sano, K.; Takagi, K.; Oka, H. Atrophy of the ipsilateral substantia nigra following middle cerebral artery occlusion in the rat. *Brain Res.* **1990**, *510*, 154–157.
- (47) Tamura, A.; Graham, D. I.; McCulloch, J.; Teasdale, G. M. Focal cerebral ischaemia in the rat: 1. Description of technique and early neuropathological consequences following middle cerebral artery occlusion. *J. Cereb. Blood Flow Metab.* **1981**, *1*, 53–60.
- (48) Quantification of the amount of metabolites formed in these incubations was not performed.
- (49) Gribkoff, V. K.; Starrett, J. E., Jr.; Dworetzky, S. I.; Hewawasam, P.; Boissard, C. G.; Cook, D. A.; Frantz, S. W.; Heman, K.; Hibbard, J. R.; Huston, K.; Johnson, G.; Krishnan, B. S.; Kinney, G. G.; Lombardo, L. A.; Meanwell, N. A.; Molinoff, P. B.; Myers, R. A.; Moon, S. L.; Ortiz, A.; Pajor, L.; Pieschl, R. L.; Post-Munson, D. J.; Signor, L. J.; Srinivas, N.; Taber, M. T.; Thalody, G.; Trojnacki, J. T.; Wiener, H.; Yeleswaram, K.; Yeola, S. W. Targeting acute ischemic stroke with a calcium-sensitive opener of maxi-K potassium channels. *Nat. Med.* **2001**, *7*(4), 471–477.
- (50) Kammerer, R. C.; Schmitz, D. A. Metabolism of methapyrilene by rat-liver homogenate. *Xenobiotica* **1986**, *16*, 671–680.

JM0101850